Development of genome editing technique and viability assays for *Chlorella vulgaris*

by
Caleb Seward

A thesis
presented to the University of Waterloo
in fulfillment of the
thesis requirement for the degree of
Master of Applied Science
in
Chemical Engineering

Waterloo, Ontario, Canada, 2021

AUTHOR'S DECLARATION

I hereby declare that I am the sole author of this thesis. This is a true copy of the thesis, including any required final revisions, as accepted by my examiners.

I understand that my thesis may be made electronically available to the public.

Abstract

Microalgae have significant potential as sustainable bio-factories for the production of high value compounds such as astaxanthin and for the production of commodity chemicals, like biofuels. However, the use of microalgae, like previous microbial processes, requires significant strain engineering efforts to make these processes economically viable. Currently, the lack of genetic tools for gene editing and strain engineering in the microalgae *Chlorella vulgaris*; one of the fastest growing species of microalgae, is impeding the commercialization of these processes. Building on well-established strategies used in yeast strain engineering, this work aims to develop an auxotrophic strain of *C. vulgaris* that can be used as a chassis for future strain modifications as well as establish a functional gene editing protocol for *C. vulgaris* that can be used to make further deletions and additions to the *C. vulgaris* genome. Using direct electroporation of CRISPR/Cas9 ribonucleic proteins (RNPs), 4 different sgRNA designs targeting the knock-out of the nitrate reductase gene were tested. Transformants were screened using potassium chlorate ($KClO_3$) as a negative selection agent, however no positive transformants were recovered. To optimize the electro-transformation protocol, impermeable viability probes were used. However, it was apparent that these probes did not behave as expected. To validate the use of several commonly used fluorescent probes in *C. vulgaris*, their performance in staining live and heat killed cells was observed by fluorescence microscopy, flow cytometry, and fluorimetry. Results indicated that fluorescein diacetate (FITC) and Sytox Green are reliable stains for viability assays in *C. vulgaris*, while propidium iodide (PI) cannot be used in this species. It is suggested that PI should not be used for viability assays in any species of microalgae as the emission spectra of PI overlaps with the maximum absorbance wavelength of chlorophyll A and B and cellular chlorophyll content can vary considerably in a single species due to changes in lighting, growth medium, and with culture age.

Acknowledgements

Foremost, I would like to thank my Supervisor, Dr. Valerie Ward, for her constant support and guidance throughout my project. I could not have done it without her support, and for that I am eternally grateful.

I would like to thank all of those in the Bio research group, especially Dr. Marc Aucoin, for taking interest in my research and providing valuable ideas and insights. I thank those in the Ward lab: Derek Kabernick, Hamid Hamedaani, Sepandar Malekghasemi and Jared Roth for their continual support and guidance during my Masters.

I would also like to thank the Aucoin, Legge and Chou labs for their permission and trust to use their lab spaces and equipment for my research.

Additionally, I would like to thank the University of Waterloo for my awarding me scholarships which allowed me to focus on my research and education.

Table of Contents

List of Figures

List of Tables

List of Abbreviations

Abbreviations

Chapter 1 – Introduction

1.1 Introduction

Microalgae have significant promise as sustainable bio factories for the renewable production of bulk and specialty chemicals. They can be grown in a carbon neutral process using inorganic carbon and nitrogen sources at mild temperatures making them potentially more sustainable than agricultural based processes (Panahi et al., 2019). However, for microalgae biomanufacturing to be economically viable, strains that are more amenable to industrial production processes must be engineered. Furthermore, competition from low-cost chemical synthesis processes play an important role in the successful commercialization of any biomanufacturing process. Historically, to establish an economically competitive biomanufacturing process, extensive strain engineering must be performed to increase productivities beyond those found in the wild-type strain (Widjaja et al., 2009). This process has been impeded by the lack of molecular tools for genetic modification in microalgae species.

Chlorella vulgaris is a prime target for strain engineering as it has the most established industrial cultivation process, is one of the fastest growing species of microalgae, is haploid meaning there is only one copy of each gene, has a sequenced nuclear, chloroplast, and mitochondrial genomes which is critical to successful genome editing, replicates using non-sexual process of mitosis, and can be grown on glucose, acetate, or phototrophically which can accelerate the gene editing process (Ru et al., 2020).

Research has demonstrated that nuclear integration of DNA is necessary in the closely related model algae species, *Chlamydomonas reinhardtii*, since the nucleus is unable to stably maintain episomal DNA (León-Bañares et al., 2004). Conversely, stable chloroplast transformation with plasmid DNA is possible as chloroplasts are prokaryotic in origin (Kindle et al., 1991). However, chloroplast transformation is limited to applications where the gene being edited is in the chloroplast genome, when chloroplast expression is desired, or when protein post translational modifications (PTM) like glycosylation are not required (Kindle et al., 1991). Therefore, tools for nuclear genome editing are necessary to undertake meaningful strain engineering projects in species of microalgae.

To date, most reports of successful genome editing in *C. vulgaris* resulted in random integration of the introduced DNA into the nuclear genome (Lau et al., 2017). However, this is undesirable as gene expression can be affected by proximal elements in the host genome resulting in different expression profiles in each mutant generated which would then necessitate extensive screening processes. Since the invention of CRISPR/Cas9 gene editing tools which allow precisely directed cuts at a specific DNA sequence, CRISPR has been successfully applied to several microalgae species using one of two methods: a plasmid-based approach, or the ribonucleic protein (RNP) approach (Y. T. Zhang et al., 2019). Both approaches require

the successful integration of the foreign DNA into the nuclear genome using one of two cellular DNA repair mechanisms: homology directed repair (HDR), or non-homologous end joining (NHEJ) (Y. T. Zhang et al., 2019). The development of a precise method for nuclear genome editing in *C. vulgaris* would allow researchers to make reproducible genetic changes including gene deletions or insertions which would open the door for more applied research into heterologous protein production, strain engineering, metabolic engineering, as well as discovery-based studies to study various biological processes in this important species.

1.2 Hypothesis

It is hypothesized that the CRISPR-RNP method recently demonstrated in other microalgae species can be successfully adapted for nuclear genome editing in *C. vulgaris*. It is further hypothesized that by transforming RNPs targeting either the coding sequences (CDS) of tryptophan synthase or nitrate reductase into *C. vulgaris*, the RNPs will create double stranded breaks at the target sites which are repaired by the cell using NHEJ which in some cases will result in the interruption of these genes, generating auxotrophic strains. Finally, the discovery that some cell viability probes do not function correctly in *C. vulgaris* resulted in a third hypothesis that chlorophyll A and B present in algal cells will absorb light emitted by fluorescent probes if their emission spectrum overlaps with the absorption spectrum of the chlorophylls present resulting in irreproducible results.

The primary objective of this work it to develop a functional CRISPR-RNP system for *C. vulgaris* and generate an auxotrophic strain. The long-term objective is to use the auxotrophic strain(s) to study the expression in heterologous genes inserted precisely into the *C. vulgaris* genome using a rational approach. To achieve the first objective, several single guide RNAs (sgRNAs) will be designed targeting different sites in the coding regions of the nitrate reductase gene. The sgRNAs will be produced using *in vitro* transcription, combined with purified Cas9 protein to form the RNPs, and the sgRNA designs will be tested using the *in vitro* Cas9 cleavage assay. RNPs will then be transformed into *C. vulgaris* using electroporation and after a recovery period, the cells will be plated on a selective agar to select for positive transformants. Positive transformants will be confirmed by their growth in ammonia containing growth medium and their lack of growth in nitrate containing media to confirm phenotype, followed by sequencing of the cut site locations to confirm genotype.

1.3 Research objectives

The objective of this research are:

1. To develop a genome editing technique to make stable nuclear edited cell lines of *C. vulgaris*. A sub-objective is to create an auxotrophic strain of *C. vulgaris* that can be used as a chassis for future genome editing studies.
2. Develop and optimize a viability assay for *C. vulgaris* that produces consistent and reproducible results
3. To confirm the cellular localization of common fluorescent viability probes in *C. vulgaris*

Chapter 2 – Literature Review

Microalgae are unicellular photosynthetic microorganisms living in freshwater or saline environments that convert sunlight, carbon dioxide and water into energy, biomass and oxygen (Panahi et al., 2019). They can be either prokaryotic or eukaryotic and are used as production platforms for high value compounds like astaxanthin and as a high protein nutritional supplement for people and livestock. Benefits of using microalgae over plants for producing high value compounds include higher growth rates, lower footprint, and lower water requirements. Microalgae have been investigated heavily recently for their ability to produce biodiesel due to high photosynthetic efficiency, higher growth rates and higher biomass production compared to other organic sources (Widjaja et al., 2009).

2.1 Chlorella vulgaris

Chlorella vulgaris is a eukaryotic fresh water green microalgae used widely in industry as a dietary supplement or protein rich food additive (Widjaja et al., 2009). It was first discovered in 1890 by the Dutch microbiologist Dr. Martinus Willem Beyerinck, and has the ability for rapid growth under mixotrophic, auxotrophic and heterotrophic conditions (Ru et al., 2020). *C. vulgaris* is 2 to 10 µm in diameter, spherical, ellipsoid or subspherical in shape and without a flagellum (Ru et al., 2020). It appears as single cells or can form colonies of up to 64 cells (Ru et al., 2020). As a non-motile microalgae, *C. vulgaris* reproduces by auto sporulation as seen in Figure 1 (Ru et al., 2020). This is a form of asexual reproduction in which the mother cell divides into 2-32 autospores, or daughter cells. When the daughter cells are mature, the mother cell wall bursts and becomes food for the daughter cells (Ru et al., 2020).

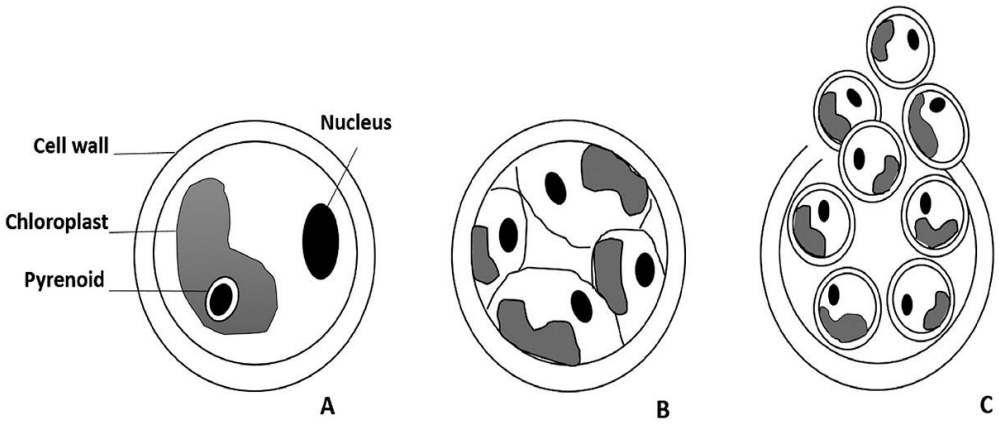

Figure 1 - Autosporulation process of *C. vulgaris.* Reproduced from (Ru et al., 2020). Permissions requested.

2.2 Biochemical Composition of *C. vulgaris*

C. vulgaris has gained attention in the biotechnology space to produce biodiesel or other high value compounds such as pharmaceuticals, which are classified as secondary metabolites (Ru et al., 2020). Primary metabolites are compounds usually essential for growth and the product of main metabolic processes such as photosynthesis and respiration (Guedes et al., 2011). Secondary metabolites are compounds produced from primary metabolites when exposed to certain environmental conditions. For example, Chlorella sp. produce lipids, a primary metabolite when the culture medium is deficient in nitrogen (Imamoglu et al., 2009). Microalgae are mainly composed of lipids, proteins, carbohydrates, minerals, and vitamins. Lipids play an essential role in growth and metabolism by acting as an energy and carbon storage reservoir. *C. vulgaris* has a lipid content that ranges from 5 to 58% of its dry weight (Safi et al., 2014). Proteins are the major constituent in most microalgae in which 20% are bound to the cell wall, 50% are within the cell and 30% are constantly moving in and out of the cell (Ru et al., 2020). Proteins have many functions in the cell including acting as enzymes, structural support and signaling. *C. vulgaris* has a protein content of 43-58% of its dry weight depending on growth conditions (Ru et al., 2020) while the carbohydrate content of *C. vulgaris* can encompass 12-55% of its dry weight (Ru et al., 2020).

2.3 Organization of the *C. vulgaris* genomes

C. vulgaris is a haploid organism that divides by autosporulation, a form of mitosis (Ru et al., 2020). It has a relatively small genome (38.8 Mb) organized into 16 chromosomes that can be easily separate by pulsed-field gel electrophoresis (Higashiyama et al., 1995). *C. vulgaris* has three separate genomes located in the nucleus (10 724 genes), chloroplast (121 genes), and mitochondria (48 genes) (Cecchin et al., 2019).

2.4 Applications of *C. vulgaris derived products*

The cultivation of *C. vulgaris* has applications in agriculture, the food industry, biofuel, aquaculture and in the pharmaceutical industry (Ru et al., 2020). *C. vulgaris* is being used in agriculture as a biofertilizer due to its high amino acid content which aid with the penetration and absorption of micronutrients through various parts of plants (Ru et al., 2020). This is because the amino acids act as chelating agents and phytosiderophores enabling the formation of stable water-soluble metal ion complexes which the plant easily absorbs. Due to its high protein content and presence of essential nutrients *C. vulgaris* is also used in the food industry as a food supplement in countries such as China, Japan, and Europe (Mata et al., 2010). *C. vulgaris* has also been cultivated for biofuel production, however it is not economical due to the high costs associated with drying and converting the algae biomass to biofuel (Hu et al., 2008). In the aquaculture industry, *C. vulgaris* is used as a nutritional supplement due to its ideal nutritional composition for fish, high digestibility and carotenoid content which improves the pigmentation of the flesh of salmonid fish

(trout and salmon) (Gouveia et al., 2003). In the pharmaceutical industry, *C. vulgaris* is gaining popularity for its high content of β-1,3-glucan which has therapeutic properties such as free radical scavenging and reduction of blood lipids in the human body (Safi et al., 2014). It is also being investigated for its application as a skin care product, as extract derived from *C. vulgaris* was found to stimulate the production of skin collagen, reduce wrinkles and slow down the ageing process (Spolaore et al., 2006).

2.5 Cultivation of *C. vulgaris*

For optimal production of high value compounds in *C. vulgaris* there are several parameters that need to be taken into consideration such as temperature, light intensity/spectra, pH, carbon source, nitrogen source and the cultivation condition (Ru et al., 2020). Temperature has a significant effect on microalgae cultivation because both photosynthesis and respiration are temperature dependent processes. The optimal temperature for *C. vulgaris* cultivation is 30°C for the highest biomass production, and 25°C for the highest lipid production levels (Kumar et al., 2010). The quality and duration of light exposure also plays a large role in *C. vulgaris* cultivation because of its role in photosynthesis. The optimal light intensity for *C. vulgaris* is 62.5 µmol photons m^{-2} s^{-1} supplied under a photoperiod of 16:8 (light: dark) cycle (Khoeyi et al., 2011). The optimal pH for *C. vulgaris* is between 10 and 10.5 (De Morais et al., 2015). The optimal nitrogen and carbon sources for *C. vulgaris* depend on the culture condition. Under mixotrophic cultures, urea is the preferred nitrogen source and glucose as the carbon source (Kong et al., 2013). Under autotrophic culture conditions *C. vulgaris* prefers ammonium as the nitrogen source and sodium bicarbonate as the carbon source (Kong et al., 2013). For culture conditions, *C. vulgaris* shows optimal growth when agitated at 250 rpm while aerated at an intensity of 200 ml/min (Mujtaba et al., 2012). One method being investigated for enhancing growth rate as well as high value product formation in *C. vulgaris* is utilizing CRISPR/Cas9 for genome editing (Jeon et al., 2017).

2.6 Cloning Techniques in Microalgae

Microalgae cloning techniques have expanded in recent years due to the potential applications in several important industries. Microalgae (with the exception of *Phaetodactylum tricornutum* (Slattery et al., 2018)) are not known to maintain episomal DNA such as plasmids or artificial chromosomes (Doron et al., 2016). Therefore, to make any permanent genetic modifications, these changes must be made directly to one of the host genomes (nuclear, mitochondrial, chloroplast). The process of genome editing can be divided into three distinct parts (i) delivery of DNA and/or small molecules into the cell needed for genome editing (transformation), (ii) method of genome editing/recombination, and (iii) selection of the positive transformants.

Selection of the genome to edit depends on the end application. Chloroplasts are prokaryotic, meaning they can be transformed with plasmids and maintain plasmids; however, protein expression is mainly limited to the chloroplast compartment (Specht et al., 2010). The chloroplast also has a more active system for homologous recombination making it easier to make genomic changes but chloroplasts lack the machinery necessary for protein glycosylation (Specht et al., 2010). The nuclear genome allows expression of proteins in any cellular compartment as well as has full post-translational machinery available to glycosylate or process proteins further, however, the efficiency of homologous recombination is low which makes it difficult to make changes to the genome (Slattery et al., 2018). These differences are summarized in Table 1. First let's discuss the delivery of DNA into *C. vulgaris* cells.

Table 1 - Microalgae protein production locations

Location of protein production	Post translational modification	Protection from proteolytic degradation	Recombinant protein production levels	Homologous recombination efficiency	Reference
Nucleus	Yes	No	Low (0.2% total soluble protein)	Low	(Doron et al., 2016)
Chloroplast	No	Yes	High (5-10% total soluble protein)	High	(Doron et al., 2016)

2.6.1 Transformation of *C. vulgaris*

There are several methods used to transform DNA into *C. vulgaris*, many which were derived from more established plant cell engineering methods including: ballistic bombardment, polyethylene glycol (PEG) mediated transformation of protoplasts with glass beads, electroporation, and agrobacterium mediated transformation. A summary of the different techniques is shown in Table 2 (Ng et al., 2017).

Table 2 - Microalgae transformation methods. Replicated from Ng et al., 2017.

Criteria	Bombardment	Glass beads	Electroporation	Agrobacterium
Technical difficulty	Low	Low	Medium	High
Equipment cost	High	Low	High	High
Predominant type of transformation	Chloroplast	Nucleus	Nucleus	Nucleus
Removal of cell wall required	No	Yes	No	No

Ballistic bombardment is primarily used for the transformation of the chloroplast. DNA is affixed to metal nanoparticles which are shot at high speeds to the host cells using a gene gun or ballistic device (Sanford, 1990). However, this device is rather expensive, and transformation of multiple genomes can occur (Sanford, 1990). However, this device can overcome the challenge of the cell wall impeding transformation and is used extensively in plant cell studies. Like plant cells, *C. vulgaris* has a thick cell wall

(17-21 nm) is mainly composed of a polysaccharide and glycoprotein matrix (Yamamoto et al. 2004; Safi et al. 2014). There is some evidence that pre-treatment with a lysozyme and sulfatase mixture increased the permeability of the cell wall of *C. vulgaris* to 96.8% (Gerken et al., 2013) without affecting its cellular viability. The addition of lysozyme results in a thinning and delaminating of the outer wall and loss of hair-like fibers from the surface of the cell as seen in Figure 2 which then allows for sulfatase to interact with the surface of *C. vulgaris* (Kumar et al., 2018).

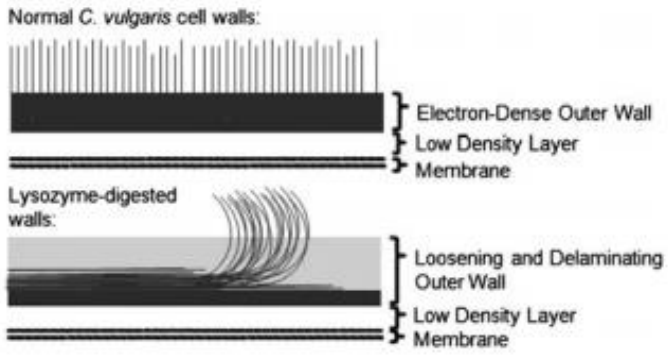

Figure 2 - *C. vulgaris* cell wall, replicated from (Gerken et al., 2013), permission requested

Protoplasting as described previously can be used with PEG and glass beads to increase transformation efficiency even further (Abidin et al., 2020). The use of PEG induces DNA uptake into cells through the interaction between DNA and the cell surface. The glass beads are used to rupture the cells so that the DNA can enter the protoplasted cells. This transformation method is low cost; however, it is more time consuming due to the protoplasting step (Abidin et al., 2020).

Electroporation is a tool used for temporarily permeabilizing cell membranes and cell walls for delivering exogenous DNA (Kumar et al., 2018). Electroporation settings such as voltage, resistance and capacitance can be altered for different cell types to ensure high transformation efficiency and cell viability. Furthermore, the electric pulse can be delivered as an exponentially decaying pulse or a square form pulse (constant for given time interval). A review of electroporation settings used in the literature for transformation of *C. vulgaris* and related species is summarized in Table 3.

Table 3 - Electroporation settings used for microalgae transformation (0.2 cm cuvettes)

Species	Pulse type	Electroporation Settings	Voltage	Reference
C. vulgaris	Exponential	25 μF, 100 Ω	360 V	(Ji & Fan, 2020)
C. vulgaris	Exponential	25 μF, 200 Ω	3300 V	(Fan et al., 2015)
C. vulgaris	Exponential	25 μF, 200 Ω	1000 V	(Abidin et al., 2020)
C. vulgaris	Square form	3.4 ms, 1 pulse	655 V	(Kumar et al., 2018)
C. pyrenoidosa	Exponential	25 μF, 100 Ω	360 V	(Ji & Fan, 2020)
C. pyrenoidosa	Square form	3.5 ms, 1 pulse	660 V	(Run et al., 2016)
C. pyrenoidosa	Square form	3.5 ms, 1 pulse	1600 V	(Run et al., 2016)
N. oceanica	Exponential	50 μF, 600 Ω	2200 V	(Li et al., 2020)

Finally, combining methods together such as protoplasting and electroporation can increase the transformation efficiency for *C. vulgaris*. As shown in Table 2, protoplasting followed by electroporation demonstrated the highest transformation efficiency at 1.77×10^4 colony forming units (CFU) per μg of plasmid used.

Table 4 - Comparison of *C. vulgaris* transformation methods

Method	Transformation efficiency (CFU μg^{-1})	Cell Concentration (cells/mL)	Protoplasting enzyme mixture	Reference
PEG & Protoplasting	356 ± 30	1.0×10^7	4.0% (w/v) Cellulase R-10 2% (w/v) Macerozyme R-10 0.1% (w/v) Pectinase 0.6 M sorbitol & 50 mM $CaCl_2$	(Yang et al., 2015)
Protoplasting & Electroporation	$1.77 \times 10^4 \pm 0.16$	2.0×10^6	1 mg/mL lysozyme 0.25 mg/mL of chitinase 1.0 mg/mL sulfatase 0.6 M sorbitol, 0.1% MES, 50 mM $CaCl_2 \cdot 2H_2O$,	(Kumar et al., 2018)
Electroporation	76	3.0×10^6	n.a.	(Muñoz et alz., 2018)

2.6.2 Genome editing in *C. vulgaris* and other microalgae

Genome editing typically involves two separate steps. First, the genomic DNA must be cut using several possible techniques, then the DNA must be repaired using cellular machinery. There are three major technologies used to cut DNA in eukaryotic species, clustered regularly interspaced short palindromic repeats (CRISPR) – CRISPR associated protein 9 (Cas9), transcription activator-like effector nucleases (TALENs), and zinc-finger nucleases (ZFNs) (Gaj et al., 2013). While all of these techniques allow the user

to make cuts in genomic DNA at specific sequences, use of TALENs and ZFNs is limited because their binding specificity relies on protein/DNA recognition and cannot be readily altered like the CRISPR-cas9 system (Gupta & Musunuru, 2014). For this reason, the popularity of CRISPR-cas9 genome editing has exploded.

The CRISPR-Cas9 system is composed of two main parts, the Cas9 nuclease that cuts double stranded DNA, and the guide RNA which targets the Cas9 protein to the desired cut site (Doudna & Charpentier, 2014). In bacteria, where this system was first discovered, the gRNA is composed of two parts, the crRNA and the tracrRNA which combine together to form the gRNA (Doudna & Charpentier, 2014). This system was simplified by fusing these two RNAs together to form a single guide RNA (sgRNA) that could be easily altered to change the cut site target (Butt et al., 2017). The target site called the protospacer must be carefully selected so that it is adjacent to the sequence NGG called the protospacer adjacent motif (PAM). The structure of the sgRNA and the crRNA/tracrRNA are shown in Figure 3. Since the discovery of the Cas9 protein, the targeting requirements (PAM site sequence can differ) of a number of different Cas proteins from many species of bacteria have been elucidated (Tang et al., 2019), however, Cas9 from *Streptococcus pyrogens* (spCas9) remains the most commonly used Cas protein and is the Cas protein used in this work. PAM sites for spCas9 can be readily identified in any piece of DNA using several free software available online; IDT & Benchling for example. These software packages will often also suggest the optimal protospacer sequence and calculate several quality metrics such as off-target and on-target scores relating to stability and specificity of the design respectively. High off-target and on-target scores on the Benchling gRNA design tool indicate a sgRNA design that will have limited off target activity while having a strong interaction with the target site.

Once the sgRNA is transcribed, it must be combined with the Cas9 protein to form the ribonucleic protein (RNP) complex which can together introduce double stranded breaks at target site in the DNA. After the DNA is cut, the host cell will try to repair the damage. There are two main mechanisms for repairing double stranded breaks, homologous recombination (HR) and non-homologous end joining (NHEJ) (Ji & Fan, 2020). HR uses a repair template with homologous sequences to repair the break. This method is the bases of most genome editing in bacteria where this mechanism is highly active (Vos & Didelot, 2008). Thus far, homologous recombination in microalgae is highly inefficient (Kilian et al., 2011). Non-homologous end joining does not require a repair template, and as the name describes it directly ligates the ends of the double stranded break together (Ji & Fan, 2020). This method is error prone and can sometimes result in the deletion of nucleotides which if the break is targeted to a site within the coding sequence of a gene, can result in the knock-out of the target gene (Ji & Fan, 2020). If a donor template is

provided, the donor template can also be inserted into the cut site by NHEJ with low frequency (Ji & Fan, 2020). This process can be seen in Figure 3 below (Zhang et al., 2019).

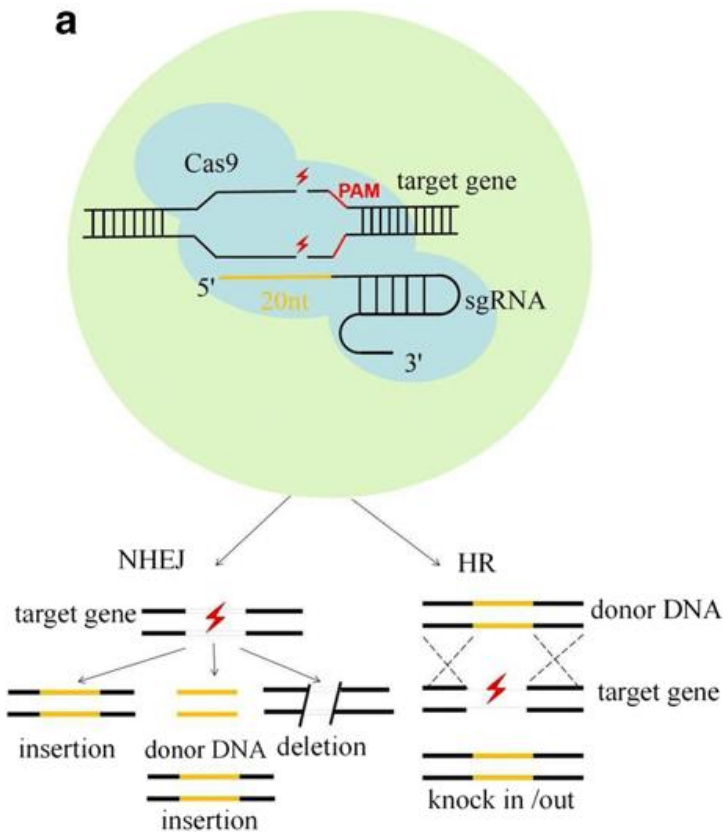

Figure 3 - Comparison of non-homologous end joining (NHEJ) and homology directed repair (HDR) repair pathways for the repair of gCRISPR-cas9 double stranded breaks in microalgae. Reproduced from (Zhang et al., 2019). Permissions requested.

There are several ways to deliver the Cas9 protein and sgRNA needed to create a double stranded break into a host cell. In many systems, Cas9 protein is expressed from a plasmid and the sgRNA is transcribed from the plasmid after transformation into the host cell (Zhang et al., 2019). Alternatively, the Cas9 protein can be purified and combined with *in vitro* transcribed sgRNA to form the Cas9 RNP complex which is delivered into the cell, as well as combinations of the two (Banakar et al., 2019). The main advantages of using the Cas9 RNP method is lower off target effects as the RNP is degraded in the cell by proteases (Seki & Rutz, 2018).

Thus far, several species of microalgae have been successfully edited using CRISPR-Cas9 including *C. reinhardtii*, *P. tricornutum* and *C. vulgaris*. Table 5 below summarizes these studies, and the highest transformation efficiency (40%) was obtained by direct transformation of CRISPR-Cas9 RNPs (Shin et al., 2016). Recently, one report of CRISPR-Cas9 mediate genome editing of *C. vulgaris* was

performed by Kim et al. (2021). In this work, the authors directly transformed *C. vulgaris* with CRISPR-Cas9 RNPs targeting Nitrate Reductase (*NR)*. It resulted in the generation of *NR* auxotrophic colonies which were selectively screened with $KClO_3$.

Table 5 - CRISPR/Cas9 experiments performed with microalgae

Species	Efficiency	Construct	Reference
N. oceanica	1 %	Plasmid	(Wang et al., 2016)
C. reinhardtii	0.1-40 %	Cas9 RNPs	(Shin et al., 2016)
P. tricornutum	31 %	Plasmid	(Nymark et al., 2016)
C. reinhardtii	10 %	Cpf1 RNPs	(Ferenczi et al., 2017)
C. reinhardtii	5-15 %	Plasmid	(Greiner et al., 2017)
C. reinhardtii	1.1 %	Cas9 RNP	(Baek et al., 2018)

2.6.3 Selection of transformants

The main methods of selection used for *C. vulgaris* in the literature are antibiotic selection (Nymark et al., 2016), and auxotrophy (Kim et al., 2021). Direct selection of transformants using a selectable marker like an antibiotic resistance gene can drastically increase the efficiency of transformation and can decrease the need for laborious colony screening. While antibiotics have been used extensively in bacteria, many common antibiotics are not compatible with eukaryotic species like *C. vulgaris*. Thus far, hygromycin and neomycin have been shown to work in *Chlorella sp.* (Lin et al., 2013). An alternative selection mechanism is auxotrophy. Auxotrophy is the inability of an organism to synthesize a particular organic compound required for its growth, this compound must be supplemented in the media. Some types of auxotrophies can be selected against by supplementing a reagent in the media that will kill non-auxotroph's. When the auxotroph gene is returned to a functional state, the strain will be able to grow on minimal media once more. This can be advantageous since supplementing antibiotics at large scale is cost prohibitive (Vidal et al., 2008). Auxotrophy is also used as a means of biocontainment as auxotroph strains will not thrive outside the laboratory (Wright et al., 2014). This means any accidental release will not result in a spread of a genetically engineered organism. Thus far, nitrate auxotrophy (inability to grow on nitrate) has been successfully used as a method of selection in genome editing in *Nannochloropsis oceanica*, and *C. vulgaris* (Poliner, 2017).

2.7 Nitrate metabolism

Nitrate assimilation is a key process for nitrogen assimilation in microalgae. First, nitrate is imported into the cell, then converted to nitrite in the cytosol, transported to the chloroplast, then converted to ammonia

(Kumar et al., 2018). Ammonia is then combined with glutamate to form glutamine which can then be used through anabolic metabolism to build other amino acids and other nitrogen-based compounds (Kumar et al., 2018). This process is shown in Figure 4. Nitrogen is vital for cellular growth, as it is required for protein synthesis and metabolic function. Nitrate reductase (NR) is the enzyme responsible for the reduction of nitrate to nitrite in the cytosol (Kumar et al., 2018).

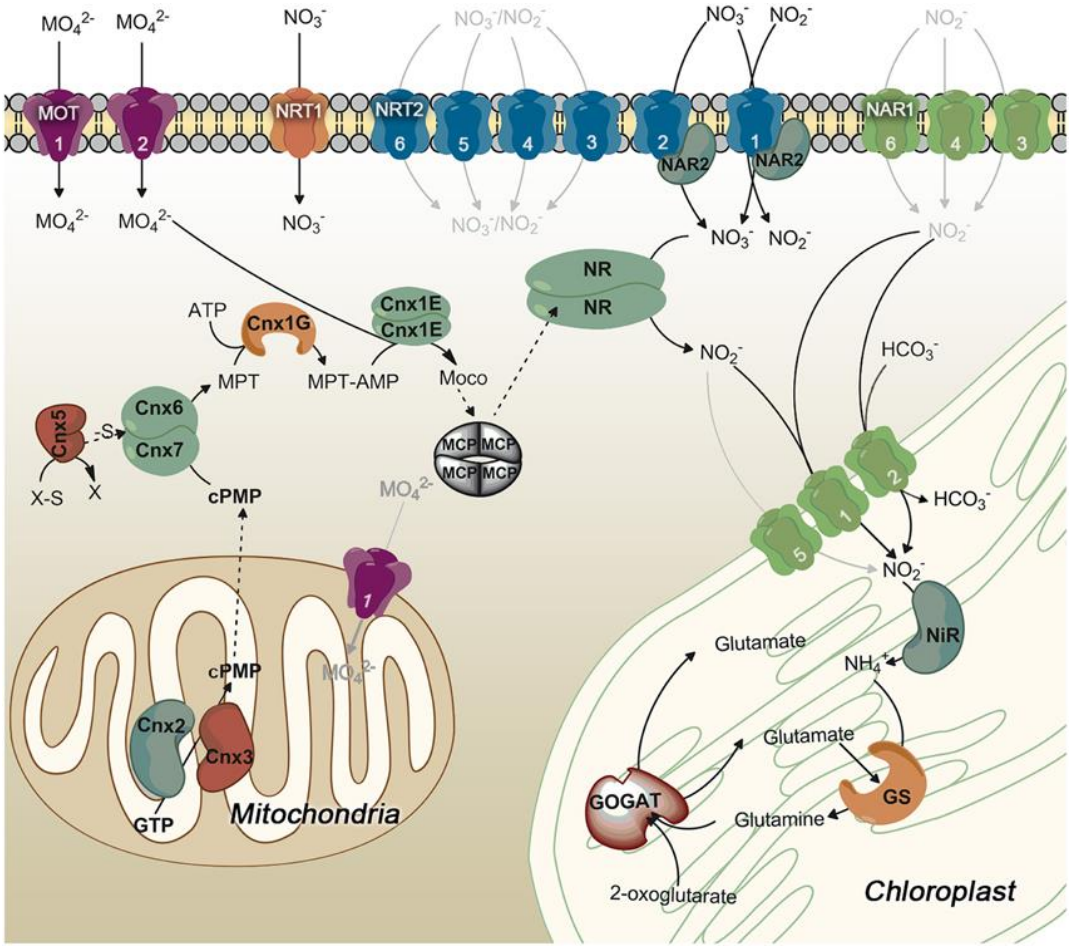

Figure 4 - Nitrogen metabolism in microalgae, nitrate is taken into the cell and converted into nitrite by nitrate reductase. then, nitrite is transported into the chloroplast and converted into ammonia which the cell can then use to make amino acids and other important biomolecules. Taken from (Kumar et al., 2018), permissions requested.

Nitrate auxotrophy can be selected for using chlorate. Cells with a functioning nitrate reductase enzyme reduce chlorate to chlorite because chlorate is an alternative substrate for the enzyme (Solomonson & Vennesland, 1972). Chlorite is toxic to the cells; therefore, wildtype cells are selected against while cells with a *NR* knockout survive. One important consideration in selecting for nitrate auxotrophs is the

repression of nitrate reductase in the presence of ammonia. To kill any cells expressing a functional *NR* gene, a nitrogen source such as nitrite must be used to prevent repression by ammonia and to induce expression of NR (Solomonson & Vennesland, 1972).

2.8 Fluorescent microscopy of microalgae

Fluorescent microscopy is a useful tool used to visualize specific fluorescent probes and has been used with *C. vulgaris* previously. One study by Yang et al, (2015) used fluorescent microscopy to visualize EGFP expression and chlorophyll autofluorescence as a measurement for transformation efficiency. Additionally, a study by Liu et al, (2007) used fluorescent microscopy to measure the effects of media iron content on lipid accumulation with the Nile Red fluorescent marker. Chlorophyll autofluorescence has also been used in fluorescent microscopy as a measurement of cell viability in a sample (Takahashi, 2019). These studies cited the fact that the presence of chlorophyll a & b in microalgae poses a challenge when performing fluorescent experiments as they can interfere with fluorescent probes with similar absorption/emission wavelengths. One of which is Propidium Iodide (PI), which has a similar emissions spectrum as shown in Table 6.

Fluorescent dyes such as PI, Fluorescein (FITC) and 5-,6-carboxyfluorescein diacetate succinimidyl ester (CFSE) have been used to measure cell viability in *C. vulgaris*. A paper by González-Barreiro et al. (2006), used PI to measure the effects of the triazine herbicides, atrazine and terbutryn on *C. vulgaris* cell viability. PI is not able to cross the membrane of live cells, therefore it is used to quantify the number of dead cells in a sample (Muñoz et al., 2018)

. This study concluded that *C. vulgaris* was superior compared to the cyanobacterium *Synechococcus elongatus* in its ability to bioaccumulate the atrazine and terbutryn herbicides while maintaining higher levels of cell viability measured with PI.

Additionally, FITC diacetate was used by Hadjoudja et al. (2009) to measure the effects of copper toxicity on cell viability in *C. vulgaris* and the cyanobacteria *Microcystis aeruginosa.* FITC diacetate is taken up by live cells and converted to its fluorescent derivative fluorescein by cellular esterase (Bono et al., 2015). Therefore, FITC diacetate fluorescence is a measure of live cells in a sample. This study concluded that *M. aeruginosa* was more sensitive to copper than *C. vulgaris* 24 hours following copper exposure measured via FITC fluorescence.

Finally, CFSE was used by Rioboo et al. (2009) to measure the effects of the triazine herbicide terbutryn on *C. vulgaris* cell division. CFSE consists of a fluorescein molecule containing two acetate moieties and a succinimidyl ester functional group. CFSE functions similarly to FITC and is used primarily to visualize cell division, as fluorescence from mother cells is redistributed equally to daughter cells. This

study concluded that terbutryn negatively impacted cell division through quantification of CFSE signaling using flow cytometry.

It is notable that none of the aforementioned studies reported that they confirmed these viability probes were acting as expected in microalgae. These probes are most commonly used in animal cell culture, and previous studies have reported issues related to optical measurements of microalgae due to the autofluorescence and broad absorption spectrum of chlorophyll (Orr & Rehmann, 2015).

Table 6 - Fluorescent Microscopy Literature Review

Dye	Excitation (nm)	Emission (nm)	Purpose	What it binds to	Final Concentration	Cell Density (cells/mL)	Reference
Fluorescein (FITC)	498	518	Stains live cells	Binds to amine and esterase substrates inside of cells	Not listed	1×10^{6}	(Bono et al., 2015)
Sytox Green	504	525	Stains dead cells	Binds to DNA, is impermeant to live cells	60 µM	1×10^{7}	(Muñoz et al., 2018)
PI	304	620	Stains dead cells	Binds to DNA, is impermeant to live cells.	60 µM	1×10^{7}	(Muñoz et al., 2018)
Acridine Orange	502	526	Stains DNA & RNA	Binds to DNA and RNA, Cell permeable	Not listed	Not listed	(Huarachi-Olivera et al., 2018)
Calcofluor White	380	475	Stains cell walls	Binds to β(1-3) and β(1-4) polysaccharides present in microalgae cell walls	Not listed	Not listed	(Coelho et al., 2019)
Chlorophyll a	372 & 642	671	NA	NA	NA	NA	NA
Chlorophyll b	453 & 643	644	NA	NA	NA	NA	NA

Chapter 3 – Materials and Methods

3.1 Materials

All cloning materials were purchased from New England Biolabs (NEB) unless otherwise indicated, while culture media was purchased from Fisher-Scientific or BioBasics. All chemicals purchased were ACS grade or above.

3.2 Strains and cultivation conditions

C. vulgaris strain UTEX 395 was purchased from the University of Texas Culture Collection. *C. vulgaris* was grown at 25 °C at 150 rpm under cyclic illumination consisting of 16 h on/8 h off in either sterile tris-acetate phosphate (TAP) media, Bold's basal medium (BBM), or BG-11 media. All media was sterilized by autoclaving at 121°C for 20 min. Seed cultures were prepared in TAP media and grown for 48 h before use. Cultures were inoculated at 10% v/v using the seed culture after removing the spent media by gentle centrifugation at 2000 × g for 5 minutes (Orr & Rehmann, 2015). TAP medium consisted of 20 mM Tris base, 1.58 mM K_2HPO_4, 2.4 mM KH_2PO_4, 7.0 mM NH_4Cl, 0.83 mM $MgSO_4$, 0.34 mM $CaCl_2$, 1 mL L^{-1} glacial acetic acid, and 1 mL L^{-1} of Hutner's trace elements solution (Hutner et al., 1950). BBM media consisted of 2.94 mM $NaNO_3$, 0.17 mM $CaCl_2 \cdot 2H_2O$, 0.3 mM $MgSO_4 \cdot 7H_2O$, 0.43 mM K_2HPO_4, 1.29 mM KH_2PO_4, 0.43 mM NaCl, 0.0027 mM $Na_2EDTA \cdot 2H_2O$, 1.8mM $FeSO_4 \cdot 7H_2O$, trace metal solution, 0.13mM H_3BO_3 and F/2 vitamin solution (Stein, 1973). BG-11 consisted of 17.6 mM $NaNO_3$, 0.23 mM K_2HPO_4, 0.3 mM $MgSO_4 \cdot 7H_2O$, 0.24 mM $CaCl_2 \cdot 2H_2O$, 0.031 mM citric acid$\cdot H_2O$, 0.021 mM ferric ammonium citrate, 0.0027 mM $Na_2EDTA \cdot 2H_2O$, 0.19 mM Na_2CO_3, 1 mM sodium thiosulfate pentahydrate (agar media only) and BG-11 trace metals solution (Du et al., 2012). When necessary 1.5% w/v agar was added to the above media to make agar plates. *E. coli* NEB-5α was used for cloning purposes and grown at 37°C at 150 rpm in LB media (10 g/L tryptone, 5 g/L yeast extract, 10 g/L NaCl). It was stored in a glycerol stock (15% v/v) at -80°C until needed. Where necessary, antibiotics were stored filter sterilized at -20°C as 1000 × stock solutions and added to agar or liquid cultures as needed.

3.3 Cell counts

Cell density was regularly measured using one of two methods, optical density measurement using a plate reader to measure the absorbance of a microplate well filled with 100 µL of culture at 680 nm for algae (OD_{680}) and 600 nm for bacteria (OD_{600}) (BioTek), or by direct count using a hemocytometer. For direct

counts, 30 µL of cell mixture was loaded onto a haemocytometer and 3 separate counts were taken for each sample and averaged to determine cell concentration.

3.4 sgRNA design

To design the sgRNA, the *NR* gene from *C. vulgaris* UTEX 259 [Accession #EF201807] was blasted against the *C. vulgaris* UTEX 395 genome. The coding sequence from the blast result was used to design sgRNAs using Benchling's guide RNA design tool. The sgRNA sequences chosen are shown in Table 5.

Table 7 - sgRNA Designs

Design	Sequence
1	GGAGGCAGCAGCACCAGCGC
2	GCAGGCAGCCAATTGCCGCA
3	GGCGCGGCAGCAAGCAGGCG
4	GGCAGCAGCACTTTCAGCAG

3.5 sgRNA cloning

Primers were designed using NEBuilder based on the pTarget plasmid to include the 20 bp sgRNA sequence in between the T7 promoter and trRNA. Primers were ordered from IDT and PCR was performed using Q5 polymerase with pTarget as the backbone. Then, the HiFi assembly master mix was used to create 4 separate pTarget plasmids containing the sgRNA designs. The plasmids were transformed into NEB-5α cells via heat shocking then recovered in SOC (20 g/L of tryptone, 5 g/L of yeast extract, 0.5844 g/L of NaCl, 0.186 g/L of KCl, 0.9521 g/L of $MgCl_2$, 3.603 g/L of glucose and 1.2037 g/L of anhydrous $MgSO_4 \cdot 7H_2O$) for 1 h with shaking at 37°C. Colonies were screened using colony PCR primers designed to amplify the correct assembly using Taq DNA polymerase (Fisher). Briefly, a small amount of a colony was added to 10 µL of sterile water and incubated at 98°C for 15 minutes to lyse the cells. Then 1 µL of this lysate was added to the Taq PCR master mix prepared according to the manufacturers standard protocol. The PCR reactions were then run on DNA gel electrophoresis to identify positive transformants which were then cultured and mini-prepped (Geneaid) and sent for sanger sequencing to confirm the correct assembly was created (TCAG Sequencing, Sick Kids, Toronto).

3.6 Homology Plasmid Cloning

Homology plasmids were designed with 500 and 1000 BP homology regions on each side of the sgRNA cut site. Primers were ordered from IDT and were designed to amplify the homology regions and the genomic DNA was amplified with Q5 PCR. Then, the HiFi assembly master mix was used to create 4

separate homology plasmids containing the homology regions designs. Initially the goal was to make 8 plasmids, 4 with 500 BP homology regions and 4 with 1000 BP homology regions. However, only 4 were successfully made based on sgRNA 1 & 2 with 500 BP & 1000 BP homology regions. This was due to the difficulty in amplifying the genomic DNA surrounding sgRNA 3 & 4. The plasmids were transformed into NEB-5α cells via heat shocking then recovered in SOC (20 g/L of tryptone, 5 g/L of yeast extract, 0.5844 g/L of NaCl, 0.186 g/L of KCl, 0.9521 g/L of $MgCl_2$, 3.603 g/L of glucose and 1.2037 g/L of anhydrous $MgSO_4 \cdot 7H_2O$) for 1 h with shaking at 37°C. Colonies were screened using colony PCR primers designed to amplify the correct assembly using Taq DNA polymerase (Fisher). Briefly, a small amount of a colony was added to 10 µL of sterile water and incubated at 98°C for 15 minutes to lyse the cells. Then 1 µL of this lysate was added to the Taq PCR master mix prepared according to the manufacturers standard protocol. The PCR reactions were then run on DNA gel electrophoresis to identify positive transformants which were then cultured and mini-prepped (Geneaid) and sent for sanger sequencing to confirm the correct assembly was created (TCAG Sequencing, Sick Kids, Toronto).

3.6.1 Competent Cell Preparation – *E. coli*

A 500 mL culture of LB media was inoculated with an overnight culture of NEB-5α and grown at 30°C and 200 rpm until the OD_{600} reached ~0.4. The culture was then chilled on ice for 30 minutes, split into 250 mL per bottle and centrifuged at 2000 × g, 4°C, for 15 minutes. The cell pellet was gently resuspended in 100 mL of ice-cold 0.1 M $MgCl_2$, then separated into four 50 mL centrifuge tubes. The cells were centrifuged and resuspended in 50 mL of ice-cold 0.1 M $CaCl_2$. Cells were incubated for 20 min, then collected by centrifugation again at 1000 × g, 4°C, for 15 min. Finally, each pellet was resuspended in 2 mL of 85 mM calcium chloride with 15% glycerol solution and 50 µL aliquots were stored in sterile microcentrifuge tubes at -80°C.

3.7 Gel Electrophoresis

For gel electrophoresis 1% DNA gels were made by microwaving 0.5 g of agarose (FroggaBio) in 50 mL of 1 × TAE buffer (4.84 g/L Tris base, 0.412 g/L EDTA $2H_2O$, and 1.14 mL/L glacial acetic acid). Once cooled, 2.5 µL of SafeView Classic (ABM) was added to the gel and the gel was poured into the casting equipment (Bio-rad, Mini-Sub Cell GT). Once the gel was solid it was placed in the electrophoresis cell and a 100 bp or 1 kbp DNA ladder was loaded (FroggaBio) into one lane. DNA for analysis was mixed with 6 × loading dye and added to the gel. Gels were run in TAE buffer at 90 V for 60 min. The results were observed using a blue light transilluminator pad (FroggaBio).

3.8 *In vitro* transcription

sgRNA was transcribed using the HiScribe T7 RNA polymerase kit from NEB with the guide RNA plasmids as a template. Reaction mixtures were made with 10 µL NTB buffer mix (6.7 mM each NTP final), 75 ng of template DNA, 2 µL of T7 RNA polymerase and water up to 30 µL. All components were thoroughly mixed and incubated at 37°C for 16 hours in the thermocycler. After, 20 µL of nuclease free water was added to each 30 µL tube, and 2 µL of DNAse was added and incubated for 15 minutes at 37°C. Following, RNA cleanup (NEB) was done and RNA yields were quantified using nanodrop. RNA was used immediately or was stored at -80°C.

3.9 Cas9 *in vitro* cleavage assay

C. vulgaris genomic DNA was extracted using a plant extraction kit (Genejet) and the *NR* gene was expanded using Q5 PCR to generate 3 separate genomic fragments. Cas9 RNPs were made by combining 1 µL Cas9 (NEB) with 3 µL of sgRNA (30 nM), 3 µL of NEBuffer and 20 µL of water at 25°C for 10 minutes. Then 3 µL of 30 nM genomic DNA was combined with the RNPs in four separate reactions at 37°C for 15 minutes with 1 µL of proteinase K addition afterwards at room temperature for 15 minutes. Resulting products were analyzed using gel electrophoresis.

3.10 Competent cell preparation and electroporation of RNPs into *C. vulgaris*

Competent cells were prepared by growing 100 mL of *C. vulgaris* cells in BG-11 media until the culture reached early exponential phase determined with OD_{680} measurements. The culture was resuspended at 10^8 cells/mL via centrifugation at 5000 × g for 5 minutes at 4°C. Cells were washed with hyperosmotic buffer 0.2 M sorbitol and mannitol at 4°C and incubated on ice for 1 hour. Cells were spun down at 2000 × g for 5 minutes at 4°C and resuspended in electroporation buffer 0.2 M sorbitol, 0.2 M mannitol, 0.08 M KCl, 0.005 M $CaCl_2$, and 0.01 M HEPES. Then 2 mm electroporation cuvettes were placed on ice for 10 minutes and 100 µL of the cell mixture with 2 ng of RNP was added. The cell mixture was electroporated at 660 V and 200 µF resistance. Immediately after, 5 mL BBM-Nitrite was added to the cuvettes in the flow hood and incubated in the dark for 12 hours. The cells were spun down at 2000 × g for 5 minutes at 4°C and resuspended to a higher concentration before being plated on selective BBM-Nitrite (20 mM) and $KClO_3$ (200 mM) plates. Plates were grown for 1 week and any colonies forming on the plates were analyzed further by growing them in BBM medium with ammonia or nitrate to compare growth rates.

To monitor electroporation, fluorescent dyes were delivered via electroporation. Cells were prepared in the same manner as described previously and a fluorescent dye was added to the final concentration reported in Table 8. PI was added to the cuvette prior to electroporation and FITC was added after electroporation to determine cell viability.

3.11 Protoplasting and PEG mediated transformation of RNPs

Cells were protoplasted by centrifuging at 5000 × g for 5 minutes at 4°C and resuspending them in 1× PBS buffer to remove the spent media. Cells were then spun down again at 5000 × g for 5 minutes at 4°C and resuspended in 0.9 mL of 0.6 M sorbitol, 0.6 M mannitol solution. Then, 50 µL of pectinase and 50 µL of cellulase (Sigma-Adrich) were added to the cell mixture and shaken overnight on a rotating mixer. Protoplasted cells were then observed by microscopy to determine extent of protoplasting.

Protoplasted cells were centrifuged at 1000 × g for 5 minutes at 4°C and gently resuspended in 5 mL of BBM containing 0.6 M sorbitol and 0.6 M mannitol. The suspension was incubated at room temperature for 5 minutes and centrifuged at 1000 × g for 5 minutes 4°C. The pellet was then gently resuspended in 5 mL of CS solution (BBM consisting of 0.6 M sorbitol and 50 mM $CaCl_2$). Then, 5 µg of the RNP complex was added to a 400 µL aliquot of above suspension containing approximately 1×10^8 protoplasts. After 15 minutes of incubation at room temperature, 200 µL of PNC solution (40% (w/v) PEG 4000, 0.8 M NaCl, 50 mM $CaCl_2$) was added with gentle mixing. After 30 minutes of incubation, 600 µL of selection medium (BBM with 0.6 M sorbitol, 0.05 M glucose, 1% (w/v) yeast extract and 200 mM $KClO_3$) was added and incubated at 25 °C in the dark overnight for cell recovery.

3.12 Fluorescent microscopy

Stock solutions were prepared for each fluorescent dye listed in Table 8 and working solutions for each dye were prepared daily. The final concentration chosen for each dye was based on manufacturer recommendations. To stain microalgae, actively growing *C. vulgaris* cells were spun down at 5000 × g for 5 minutes at 4°C and were resuspended to 10^{11} cells/mL. Fluorescent dye was added to the cell mixture according to Table 8 and were incubated for 15 minutes. All cell mixtures except for Sytox green were spun down at 5000 × g for 5 minutes at 4°C and were resuspended in BG-11 media to remove any excess fluorescent dye. Then, 20 µL of cell mixture was added onto microscope glass and fixed in place using an adhesive. The slides were then imaged using a Zeiss LSM 700 confocal microscope equipped with the following lasers: 488 nm (green), 555 nm (red), 639 nm (far red). The Zen software was used for post processing of fluorescent images.

Table 8 - Fluorescent dye concentrations and excitation/emissions used

Dye	Final Concentration	Laser used	Emission Wavelength
FITC diacetate	10 µg/mL	488 nm	520 nm
Propidium iodide	3 µg/mL	488 nm	620 nm
Sytox Green	30 nM	488 nm	525 nm

Calcofluor white	2 µg/mL	405 nm	475 nm
Acridine orange	2 µg/mL	488 nm	525 nm
Chlorophyll a	n.a.	372 nm	671 nm
Chlorophyll b	n.a.	453 nm	644 nm

3.13 Fluorimetry

Actively growing *C. vulgaris* cells were spun down at 5000 × g for 5 minutes at 4°C and were resuspended to 10^{11} cells/mL. Fluorescent dye was added to the cell mixture according to Table 8 and were incubated for 15 minutes. All cell mixtures except for Sytox green, were spun down at 5000 × g for 5 minutes at 4°C and were resuspended in BG-11 media to remove any excess fluorescent dye. Then, 100 µL of cell mixture was added in triplicate in a black 96 well plate and analyzed using a fluorometer (BioTek) set at the appropriate absorption/emission spectra. For experiments investigating dead cells, cells were killed via heat shocking at 75°C for 20 minutes.

3.14 Flow cytometry

Actively growing *C. vulgaris* cells were spun down at 5000 × g for 5 minutes at 4°C and were resuspended to 10^{10} cells/mL. Fluorescent dye was added to the cell mixture according to Table 8 and were incubated for 15 minutes. All cell mixtures except for Sytox green, were spun down at 5000 × g for 5 minutes at 4°C and were resuspended in BG-11 media to remove any excess fluorescent dye. Cells were fixed by adding 27 µL/mL of 37% formaldehyde and incubated for 15 minutes at room temperature. Samples were analyzed using (BD Accuri) flow cytometry using a blue and red laser and data was analyzed using FlowJo.

3.15 Chlorophyll content

Chlorophyll content was measured by mixing 0.05 g of freeze dried *C. vulgaris* in 8 mL of acetone solution (80 % (v/v) acetone, 2.5 mM sodium phosphate buffer pH 7.8) for 16 hours on a rotary shaker (Orr & Rehmann, 2014). Then, samples were centrifuged at 2000 × g for 2 minutes at 4°C with the supernatant decanted in between centrifugations for later analysis. The pellet was washed with 2 mL of acetone and was centrifuged at 2000 × g for 2 minutes at 4°C two more times with the supernatant decanted and pellet washed with 2 mL of acetone. The final volume of the collected supernatant was adjusted to 15 mL with acetone and was analyzed using a UV-Vis spectrophotometer (BioTek). Total chlorophyll content was determined using the following formula:

$$\text{Total chlorophyll content (\%w/w)} = (17.76\times[A_{645}] + 7.34\times[A_{663}]) / (\text{mass of sample})$$

Chapter 4 – Results

To begin, the *C. vulgaris* genome was searched for common auxotrophy targets using NCBI BLAST that have established negative selection methods such as tryptophan synthase. However, these genes were not annotated in the *C. vulgaris* genome nor were we able to identify any putative sequences by BLASTp using tryptophan synthase from a related model microalgae species, *C. reinhardtii*. However, it was previously reported for *Nannochloropsis* species of microalgae that nitrate reductase (*NR*) activity could be used as an auxotrophic marker after CRISPR gene editing and the *NR* gene has been identified in *C. vulgaris* (Kilian et al., 2011).

4.1 sgRNA Design

4.1.1 Identification of nitrate reductase gene

Nitrate reductase is a 100 kDa protein located in the cytosol of *C. vulgaris* (Solomonson & McCreery, 1986). The gene encoding *NR* is divided into 19 exons in the nuclear genome (Accession number MN627215.1) (Dawson et al., 1996). The gene locus was identified by blasting the *NR* gene with the *C. vulgaris* UTEX395 genome (Accession number EF201807). The *NR* gene was isolate by Q5 PCR of genomic DNA extracted from *C. vulgaris* as seen in Figure 5 below.

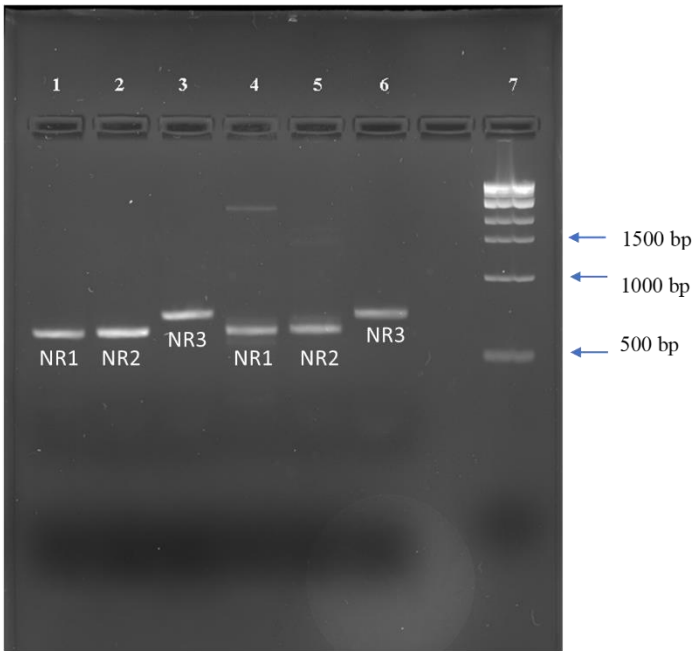

Figure 5 - *NR* genomic DNA amplified with Q5 PCR, lane 1 = *NR* region 1 (629 bp), lane 2 = *NR* region 2 (629 bp), lane 3 = *NR* region 3 (715 bp), lane 4 = *NR* region 1 (629 bp), lane 5 = *NR* region 2

(629 bp), lane 6 = *NR* region 3 (715 bp), lane 7 = 1 kb ladder (NEB).

The structure of the *NR* gene and sgRNA binding sites is shown in Figure 6 (A) below. Additionally, the sgRNA design is demonstrated in Figure 6 (B) below.

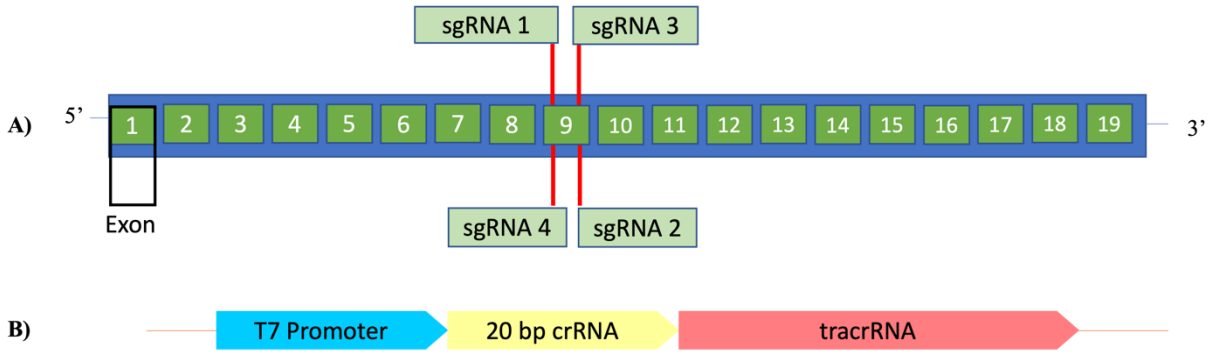

Figure 6 - A) Depiction of *NR* gene and sgRNA cut sites B) depiction of sgRNA transcription design

The coding sequence of *NR* was entered into Benchling and the PAM sites and crRNA sequences for *Streptococcus pyrogens* cas9 protein were computed. The results are presented in Table 9 below. The on-target site score indicates cleavage probability, the off-target score indicates off target effects, with a higher score for both indicating a higher quality design. For this reason, the four designs with the highest on and off target scores were chosen for cleavage of the *NR* gene with design two being the best due to its highest on-target and off target scores.

Table 9 - gRNA designs

Design	Position	Strand	Sequence	PAM	On-target score	Off target score
1	3381	antisense	GGCGCGGCAGCAAGCAGGCG	GGG	15	45
2	4672	sense	GGAGGCAGCAGCACCAGCGC	CGG	30.4	21.2
3	4134	antisense	GGCAGCAGCACTTTCAGCAG	CGG	63.2	50.1
4	3806	antisense	GCAGGCAGCCAATTGCCGCA	CGG	94	94.9

4.1.2 Cloning of sgRNA designs

To form CRISPR-RNPs *in vitro*, *in vitro* transcription is often used to produce large amounts of sgRNA quickly from a DNA template. To create a template for transcription, the T7 promoter, the crRNAs identified by analysis with Benchling, and the trRNA sequences were assembled using Gibson HiFi assembly into the plasmid pTarget. The transcription template is shown in Figure 6 (B). The T7 promoter was amplified from pET28a-Cas9-His plasmid, and the crRNA was amplified along with the pTarget backbone and overlaps were designed to add the 20 bp crRNA sequences using NEBbuilder. The assembly was transformed into NEB-5α and positive transformants were detected using cPCR. The plasmids were then sent for sequencing and the results are for the sgRNA sequences are shown in Figure 7. A representative gel of cPCR results is shown in Figure 8. The transcript for T7 polymerase was amplified using Q5 PCR and the results are shown in Figure 9.

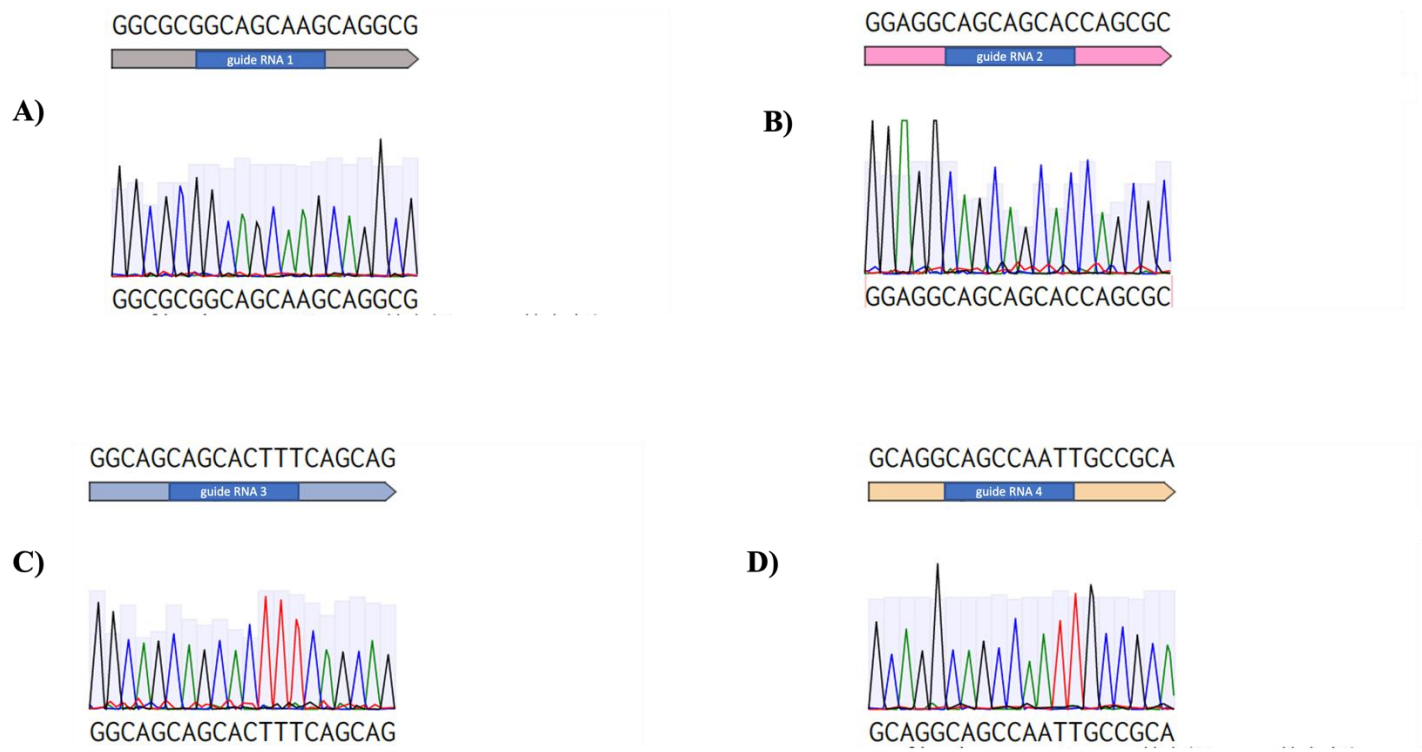

Figure 7 - Sequencing Data – sgRNA PCR. A) Sequencing data for sgRNA 1 B) Sequencing data for sgRNA 2 C) Sequencing data for sgRNA 3 D) Sequencing data for sgRNA 4

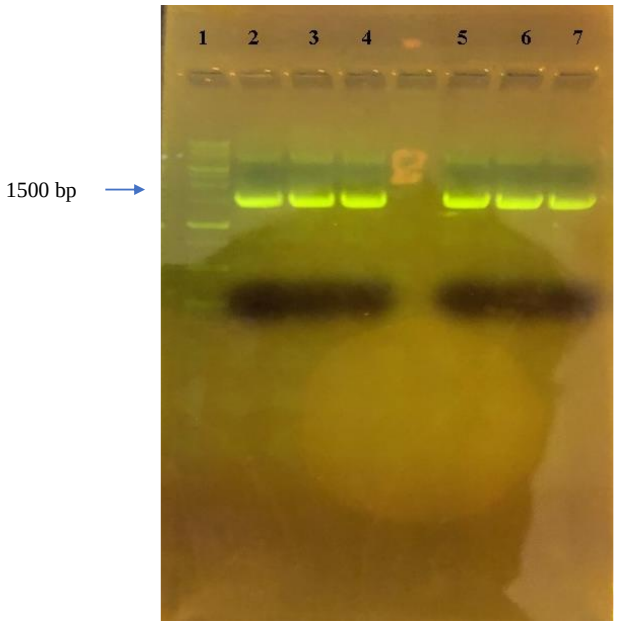

Figure 8 - Colony PCR results for sgRNA plasmids 1) 1 kb ladder 2,3,4,5,6,7) colony PCR fragments 1500 bp long indicating successful construction of sgRNA plasmids

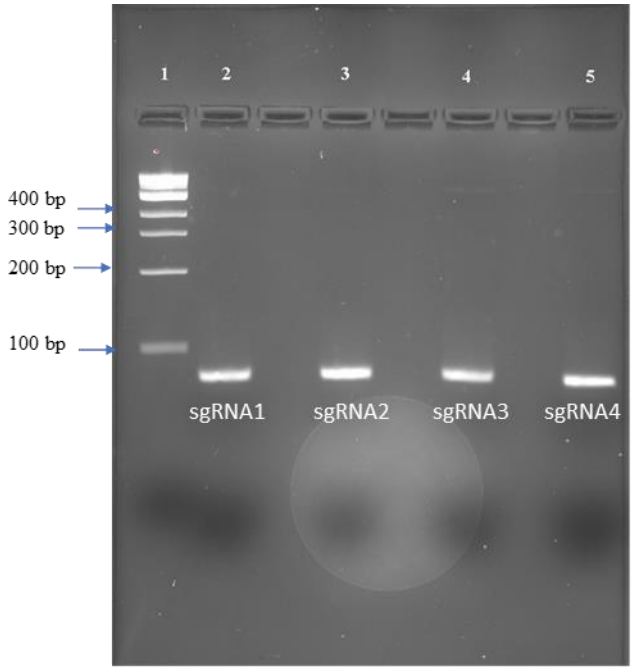

Figure 9 - sgRNA-DNA templates for *in vitro* transcription made with Q5 PCR, lane 1 = 1 kbp ladder (NEB), lane 2 = sgRNA 1 lane 3 = sgRNA 2, lane 4 = sgRNA 3, lane 5 = sgRNA 4. Expected size X bp.

4.2 Homology plasmids

In parallel, to facilitate gene knock in using HDR a template for recombination was made. Two plasmids were constructed containing either 500 bp or 1000 bp homology regions (HR) matching the regions flanking the NR cut sites. Amplification of the HRs is shown in Figure 10. A cassette for expression of eGFP using the Cauliflower Mosaic Virus (CaMV) 35S promoter, the omega leader sequence (5'UTR) from Tomato Mosaic Virus (TMV), and the nopaline synthase (Nos) terminator from *A. tumefaciens* (3'UTR), was inserted into the middle of the homology regions.

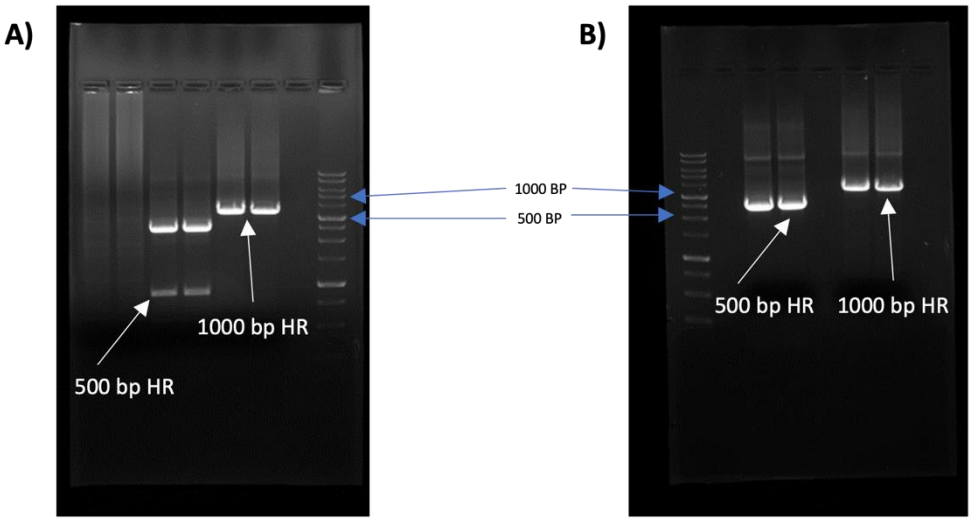

Figure 10 - Amplification of HR from genomic DNA. A) sgRNA 1, 500 BP homology band in the middle, 1000 BP homology on the right B) sgRNA 2, 500 BP homology band in the middle, 1000 BP homology on the right

4.3 sgRNA manufacturing

The efficiency of DNA digestion by Cas9 is dependent on the ratio between sgRNA to Cas9 protein due a mutualistic interaction. The sgRNA functions to guide the Cas9 protein to a specific location in the genome, and the Cas9 protein creates a double stranded break. Low sgRNA concentrations will result in unbounded Cas9 protein and a lower concentration of active RNP complexes which can reduce the efficiency of genome editing.

During the CRISPR/Cas9 *in vitro* digestion experiment, it became evident that guide RNA yields from *in vitro* transcription were lower than expected. Therefore, transcription was optimized to increase the amount of sgRNA produced. To increase the quantity of sgRNA, greater efforts were taken towards removal of RNase such as sterilization of pipettes, tips, water, as well as cleaning of surfaces with RNAse

decontamination solution RNAse Away/Zap. In addition, RNAse Off was added to the transcription reaction mixture to inactive any RNAse present. These interventions resulted in a significant increase in the quantity of RNA manufactured as seen in Table 10.

Table 10 - sgRNA production optimization

Condition	RNA Yield Prior To RNAse Off Addition	RNA Yield with Addition of RNAse Off	% Difference
sgRNA 1	1.9 ng/µL	14,236.2 ng/µL	199.9%
sgRNA 2	6.1 ng/µL	20,542.3 ng/µL	199.9%
sgRNA 3	3.5 ng/µL	14,273.7 ng/µL	199.9%
sgRNA 4	6.7 ng/µL	18,576.9 ng/µL	199.9%
Control	5.6 ng/µL	22,059.05 ng/µL	199.9%

4.4 *In vitro* RNP experiment

With the successful construction of the sgRNA plasmids, an increasing the quantity of sgRNA produced from *in vitro* transcription, an *in vitro* Cas9 digestion assay was performed. Cas9 RNP complexes (Cas9 + sgRNA) were incubated with a section of PCR amplified *NR* gene to look for evidence of digestion. The NR gene fragments were designed to digest into two easily distinguishable sizes when cut with Cas9. The results of the *in vitro* cleavage assay are shown **Figure 11**. Lanes 6-8 represent the un cleaved PCR product, and lanes 1-4 represent the sgRNA RNP fragments. The experiment did not work, as there is only one band in lanes 1-4. Whereas there should be two distinct bands in lanes 1-4 based on previous CRISPR/Cas9 experiments. The sizes of the expected digested bands are listed in Table 11.

Table 11 - Expected band sizes for Cas9 in vitro cleavage assay

Condition	Uncut fragment size	Expected sizes after digestion
sgRNA 1	629 BP	217 and 412 BP
sgRNA 2	627 BP	249 and 378 BP
sgRNA 3	715 BP	410 and 305 BP
sgRNA 4	629 BP	421 and 208 BP

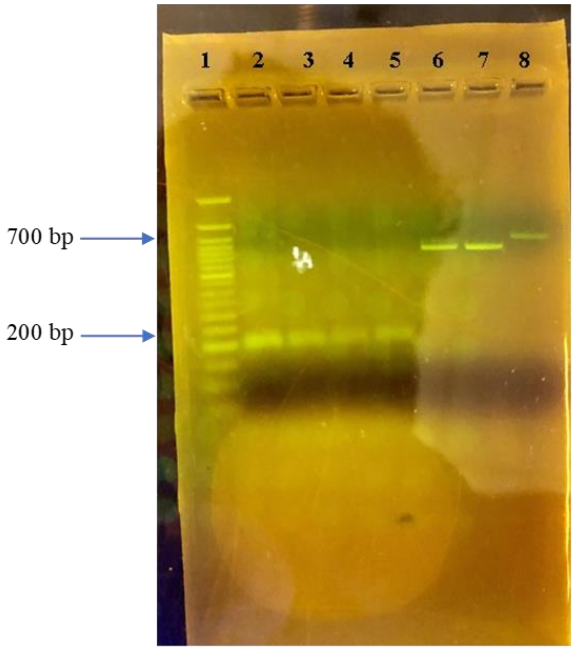

Figure 11 - *In vitro* RNP digestion results, lane 1 = 1 kb ladder (NEB), lane 2 = RNP 1 + *NR* segment 1, lane 3 = RNP 2 + *NR* segment 2, lane 4 = RNP 3 + *NR* segment 3, lane 5 = RNP 4 + *NR* segment 3, lane 6 = *NR* segment 1, lane 7 = *NR* segment 2, lane 8 = *NR* segment 3

From this assay, it was unclear if the digestion was proceeding as expected. Although there are no cleaved bands visible, over digestion with Cas9 can lead to complete degradation of the product (Cai et al., 2018) . In many reports, the cleaved fragments were less intense than the uncleaved control fragments (Cai et al., 2018). Furthermore, the RNP complexes are visible in the digestions at ~200 bp. Attempts to decreases incubation time, increase the concentration of the template, and add RNAse inhibitor to the reaction gave the same results (data not shown). Additionally, due to time constraints the homology plasmids were not tested in an *in* vitro experiment. It was therefore decided to proceed with the electroporation of RNPs for the generation of auxotrophs.

4.5 Electroporation of Cas9 RNPs

Cas9 RNPs were prepared with each sgRNA design and electroporated into *C. vulgaris* electrocompetent cells (1×10^8 cells/mL). The cells were recovered for 16 h in the dark, then centrifuged and plated onto two TAP agar plates. One plate contained ammonia as a nitrogen source and the other contained nitrate. It is expected that if auxotrophs are generated by NHEJ indels formed after Cas9 cleavage, that the number of

colonies observed on the TAP nitrate plates would be less than those found on the ammonia plates. The resulting plates are shown in Figure 12. The colony count data for each sgRNA is presented in Table 12.

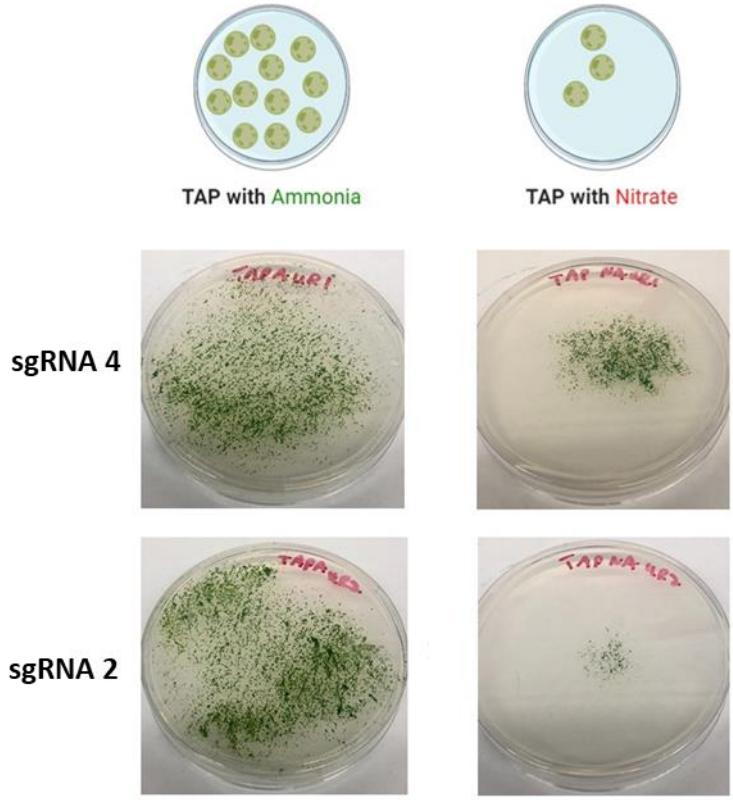

Figure 12 - Examples of transformants after electroporation with Cas9 RNPs. Transformants were plated on TAP agar plates with either ammonia (left hand plates) or nitrate (right hand plates). A visual representation of the expected results is shown above. A) sgRNA design 4, B) sgRNA design 2.

Initial experiments indicated a significant difference in the number of colonies (average colonies on nitrate= 370 ± 168, average colonies on ammonia: 510 ± 123) and this data was used to estimate the number of colonies that must be screened to identify one auxotroph strain (27.5% reduction or ~1/4). Therefore, 100 isolated colonies were replicate plated onto ammonia and nitrate plates as seen in **Figure 13** and were later grown in liquid media to confirm/deny the presence of nitrate auxotrophy.

Table 12 - Plate counts for Cas9 RNP transformants plates on TAP nitrate or TAP ammonia plates.

		Colony Count		
Sample	**Replicate**	**Nitrate Plate**	**Ammonia Plate**	**Difference**
sgRNA 1	1	376	476	100
	2	612	712	100
	3	551	651	100
sgRNA 2	1	383	559	176
	2	362	400	38
	3	19	516	497
sgRNA 3	1	359	470	111
	2	312	400	88
	3	591	714	123
sgRNA 4	1	166	446	280
	2	321	366	45
	3	379	404	25

4.5.1 Replica plating for identifying nitrate auxotrophs

Single colonies were resuspended in water and replica plated on TAP nitrate and TAP ammonia plates as seen in **Figure 13**. Colony 2 shows potential auxotrophy for nitrate as it did not grow on the nitrate plate. However, in liquid cultures it was found to grow in both nitrate and ammonia indicating this was not a true auxotroph. Therefore, it was decided that a negative selection method to remove untransformed cells would be useful in increasing the likelihood of identifying a true auxotroph.

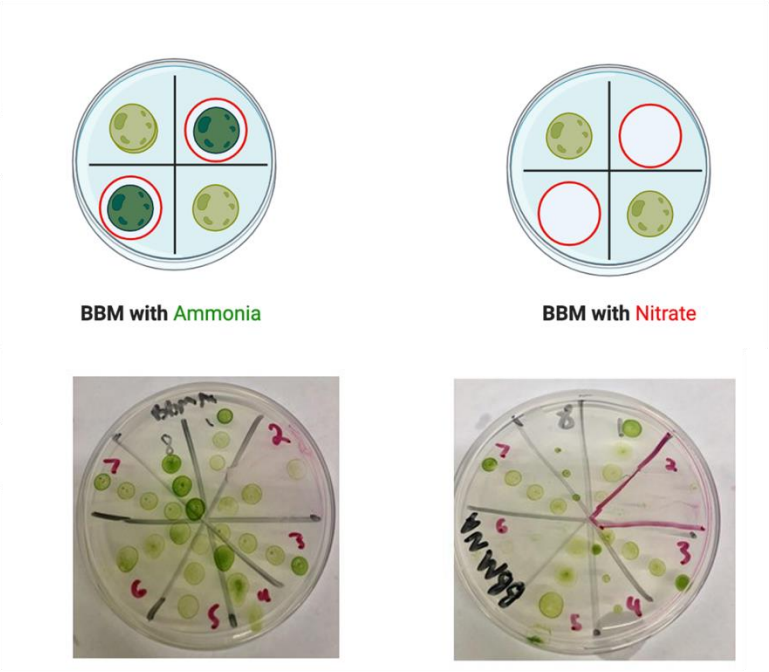

Figure 13 - Examples of replica plating of single colonies from transformant plates. Single colonies were plated onto two TAP agar plates with either ammonia (left hand plates) or nitrate (right hand plates). A visual representation of the expected results is shown above.

4.5.2 Growth of potential auxotrophs in liquid media

To confirm auxotrophy, the two colonies identified by replica plating were grown in liquid media with ammonia or nitrate. The growth over 7 days was monitored by optical density measurements for 2 colonies and compared to the growth of the wildtype strain in Figure 14. Growth was poor for the possible auxotrophs indicating they were not true auxotrophic strains.

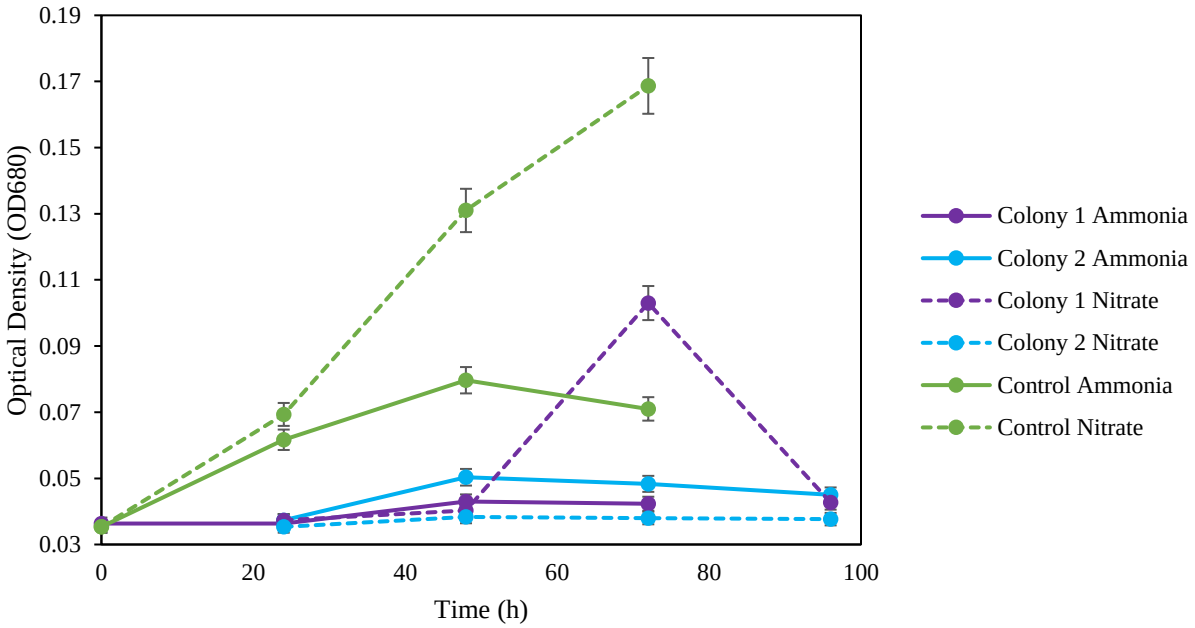

Figure 14 - Growth of two possible auxotrophs in BBM media with ammonia (solid) or nitrate (dashed). Growth of the wildtype strain is shown in green.

4.6 Use of selective media

Chlorate has been successfully used to select for nitrate auxotrophs in a variety of species (Solomonson & Vennesland, 1972) including *C. vulgaris* (Kim et al. 2021). First, the concentration of $KClO_3$ in the selection media tested to select an appropriate concentration to prevent growth of wild-type *C. vulgaris*. The optimal concentration for $KClO_3$ in the selection media is 200 mM as seen in Figure 15.

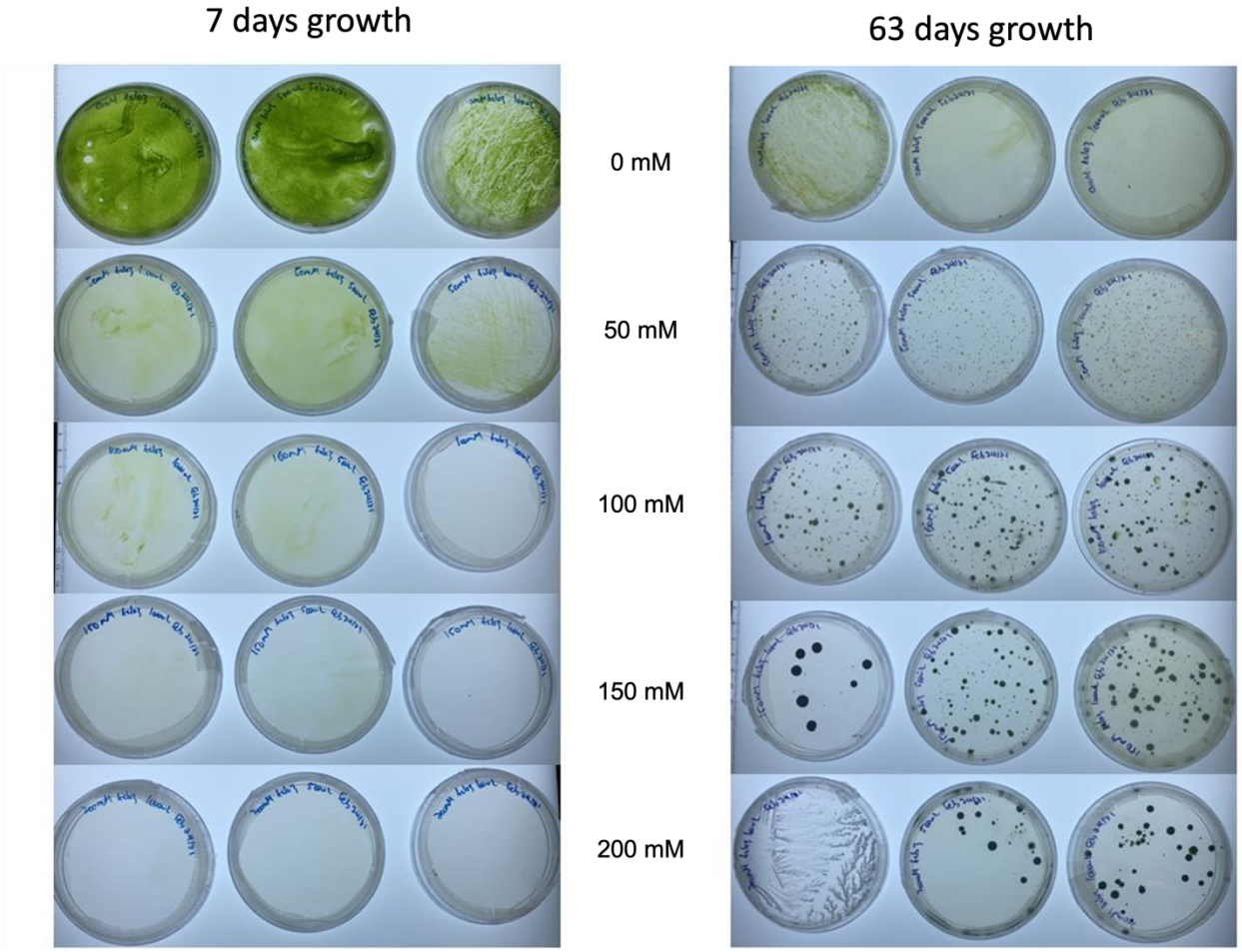

Figure 15 - Optimization of $KClO_3$ concentration in selective media. BBM plates with nitrite and $KClO_3$ inoculated with a lawn are shown after 7 days of growth (left) and 63 days growth (right).

It became apparent that $KClO_3$ selection may wane over time, possibly due to degradation, as several colonies were found to grow on the plates are 63 days of incubation. It was therefore concluded that this selection media should only be used for the first 1-3 weeks of cell growth, and cells should be transferred over to fresh plates every 1-3 weeks for efficient auxotroph selection.

4.7 Electroporation of Cas9 RNPs and recovery on chlorate selection media

The previous experiment was repeated with a higher cell density (10-fold increase, 1×10^9 cells/mL) and the transformants were plated onto the selection plates. The results are shown in Table 13.

Table 13 - Plate counts for Cas9 RNP transformants plates on BBM plates with ammonia, nitrate, and nitrite with 50 mM $KClO_3$.

Condition	Ammonia Colonies	Nitrate Colonies	$KClO_3$ Colonies
sgRNA 1 500 BP HR	4512	4403	1
sgRNA 1 500 BP HR (1/6 dilution)	3410	3323	0
sgRNA2	3439	3008	3
sgRNA 1	3713	3577	2
sgRNA 4	2598	2460	4
Electroporated control	6702	6956	0
Non electroporated control	6744	6609	0

As can be seen, the number of colonies on the $KClO_3$ plates was significantly lower than the ammonia or nitrate plates. Again, possible auxotrophs were identified by replica plating and then grown in liquid media (Figure 16). None of the possible auxotrophs exhibited growth in only ammonia indicating these colonies were not true auxotrophs.

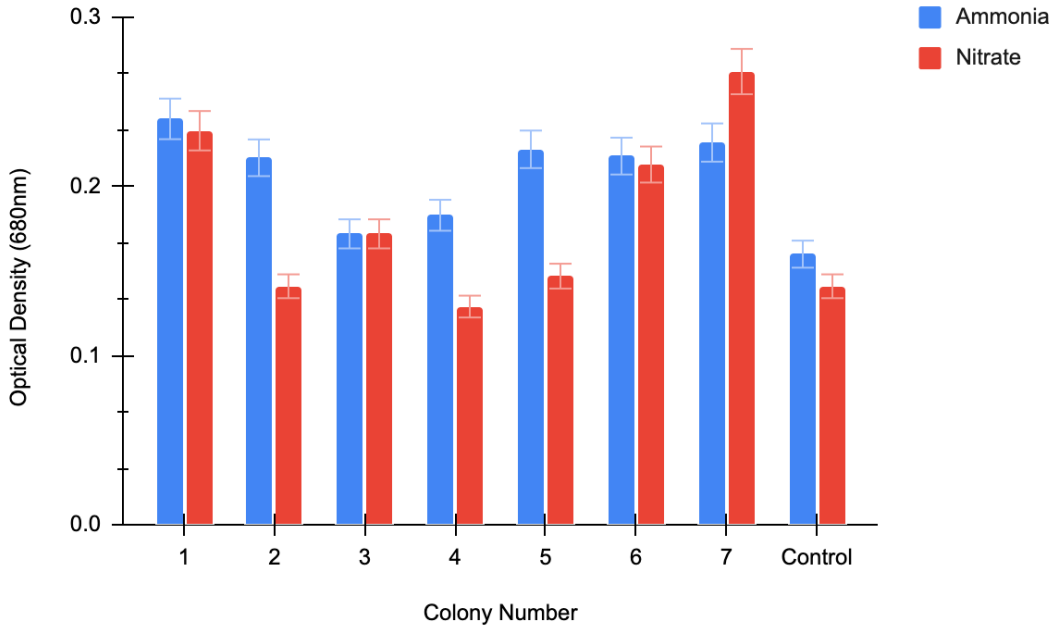

Figure 16 - Post in vitro experiment 2 growth data.

To ensure the transformants were auxotrophs, the concentration of chlorate in the recovery plates was increased (Figure 17) and chlorate was included in the post-electroporation recovery period in liquid media.

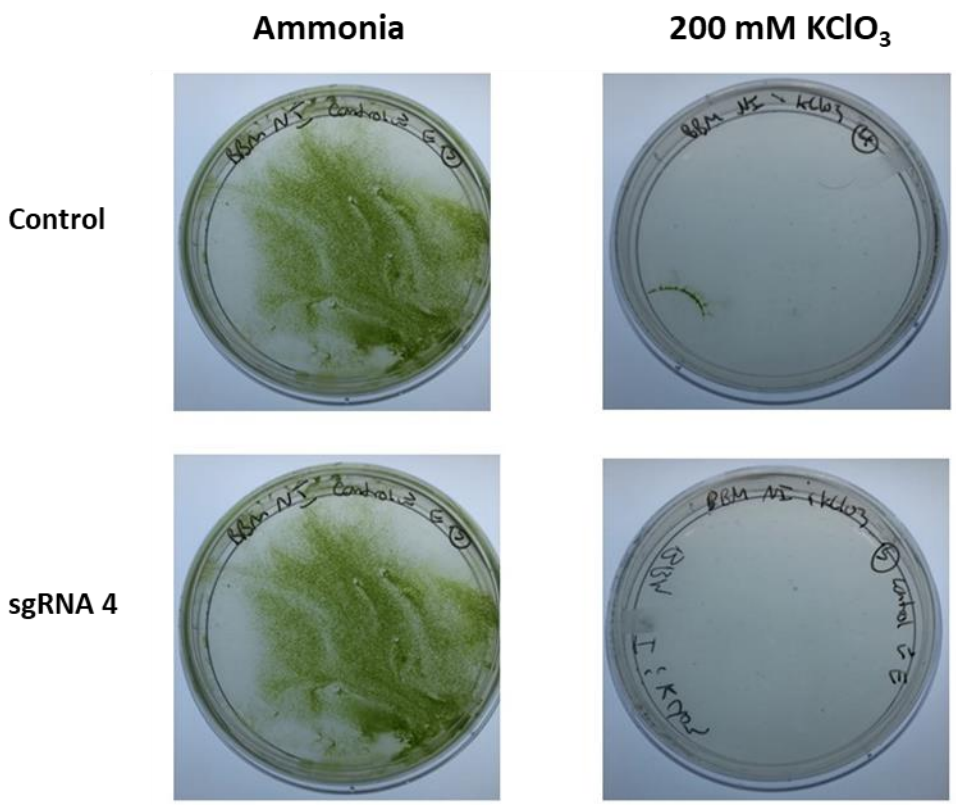

Figure 17 - Example of transformants recovered for 24h in BBM (1% glucose, 200 mM $KClO_3$) were plated on ammonia or selection plates.

Again, colonies were replica plated, then grown in liquid media.

Figure 18 shows the growth in flasks of the potential auxotrophs. Flask #2 grew in ammonia and the selection media indicating a possible auxotroph for nitrate assimilation. However, this colony did not grow in the selection media in another experiment indicating that it was not an auxotroph. Selection of nitrate assimilation auxotrophs with chlorate can potentially result to two types of mutants, (i) mutants with non-functional nitrate reductase or (ii) mutants with a non-functional nitrate transporter (Solomonson & Vennesland, 1972).

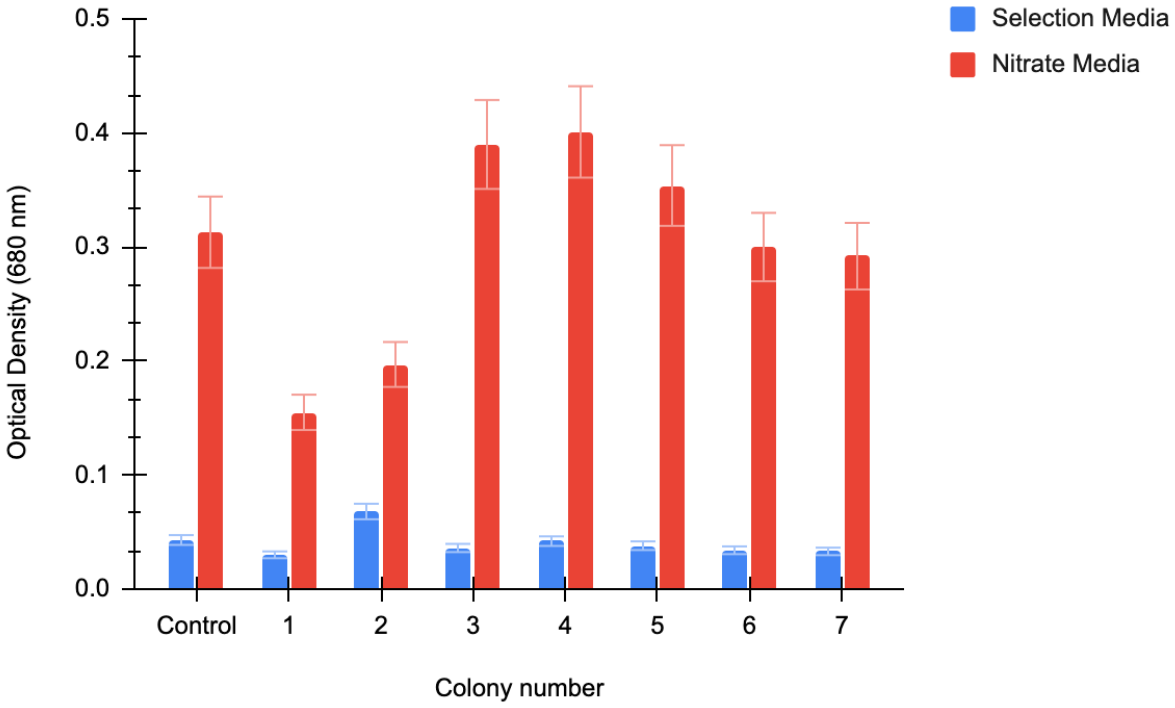

Figure 18 - Screening auxotroph growth in liquid media.

Figure 19 bellow shows the growth of colonies from the Figure 18 experiment. Colony number 2 can be seen in Figure 19 as the only colony that grew well on the selection media.

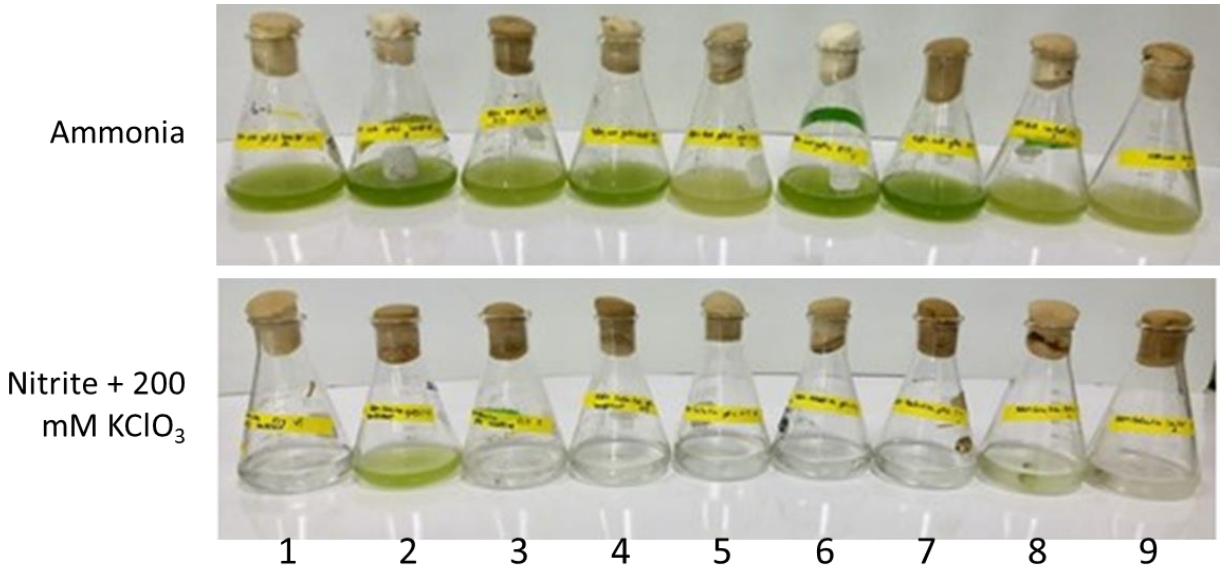

Figure 19 - Photo of growth in flasks to screen for potential auxotrophs in liquid media.

4.8 Effect of cell concentration on transformation

To increase the likelihood of obtaining a true auxotroph, the cell concentration during electroporation was increased as shown in Figure 20. A small number of colonies grew when a concentration of 1×10^{10} cells/mL was used for electroporation (Figure 20. , right).

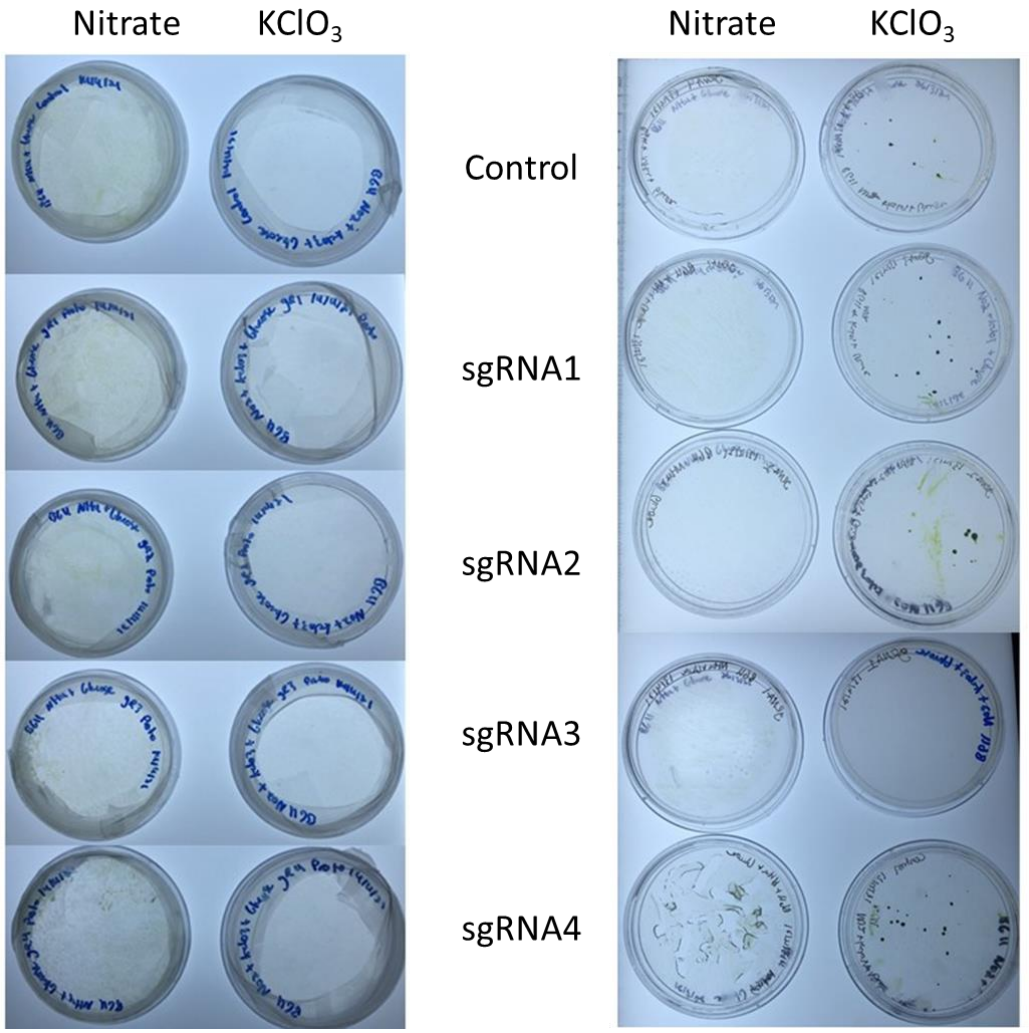

Figure 20 - Transformants plated on nitrate or selection plates with different concentration of electrocompetent cells. Left) 1×10^{9} cells/mL starting concentration Right) 1×10^{10} cells/mL starting concentration.

4.9 Optimization of recovery media

Due to the low growth rate of *C. vulgaris* cells on control agar plates containing nitrite, and the results indicating that chlorate selection degrades over time, perhaps optimizing growth on nitrite plates would result in an increased recovery of transformants.

4.9.1 Addition of organic nitrogen to nitrite plates

As chlorates are known to degrade under high light conditions (Jung et al., 2016), TAP agar plates supplemented with organic nitrogen sources were grown in duplicate with one set incubated in the dark, and one under illumination. As you can see in

Figure **21**, the plates that were put in the dark (left) did not grow very well compared to the plates that were put in the light (right). Additionally, supplementation with casamino acid resulted in higher growth rates compared to the plates with yeast extract. While *C. vulgaris* growth on TAP was in the past was higher than growth on phototrophic BBM plates due to supplementation with acetate in TAP media, growth on BBM with glucose appeared to be faster. Therefore, a similar experiment to test supplementation of organic nitrogen on BBM with glucose and nitrite. Conditions are summarized in Table 14.

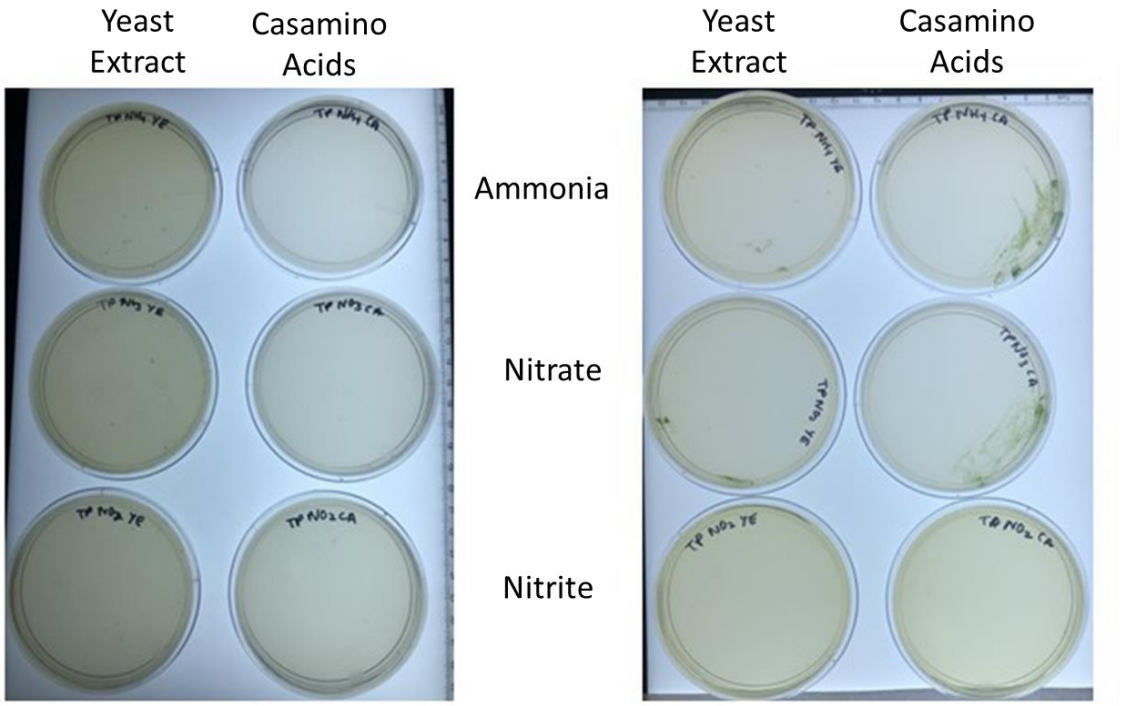

Figure 21 - Growth after 5 days on TAP plates containing ammonia, nitrate, or nitrite supplemented with 1% yeast extract or 1% casamino acids. (Left) plates grown in the dark (Right) plates grown under illumination.

Table 14 - Nitrogen sources used on BBM plates to improve growth

Condition	Nitrogen Source	Casamino acid Concentration
1	3 mM Nitrite	none
2	3 mM Nitrite	10 g/L
3	3 mM Urea & Nitrite	none
4	3 mM Urea & 3 mM Nitrite	10 g/L
5	20 mM Nitrite	none
6	20 mM Nitrite	10 g/L

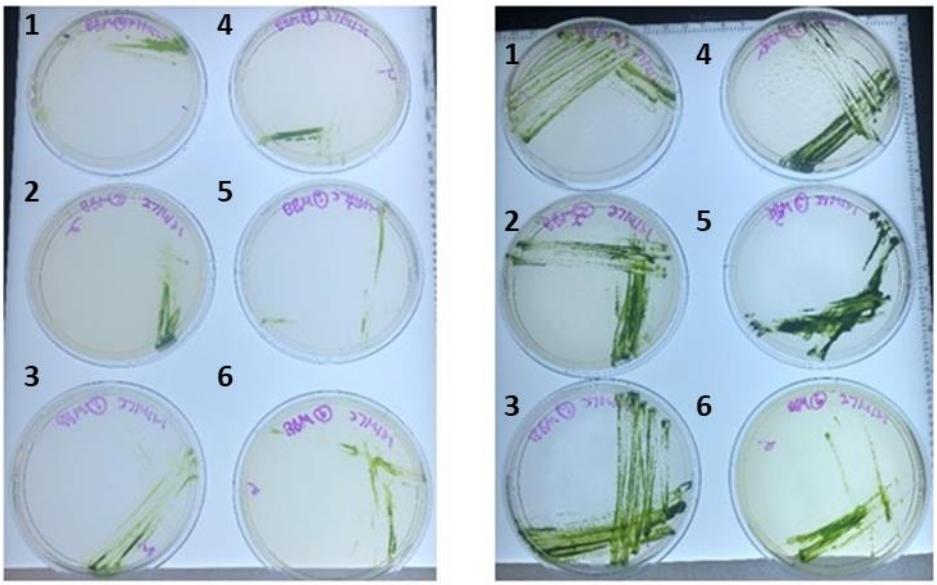

Figure 22 - Growth after 5 days on BBM plates with organic nitrogen sources (indicated by numbers 1-6) as described in Table 14. Plates were grown in either the dark (left) or under light (right).

Growth was improved when the plates were illuminated, and the colonies were darker (Figure 22). Otherwise, addition of urea, supplementation of casamino acids, and increasing the nitrite concentration from 3 to 20 mM had minor effects on growth on plates.

4.10 Optimizing electrotransformation of *C. vulgaris*

4.10.1 Electrocompetent cell preparation

Some reports used BG11 media to prepare electrocompetent *C. vulgaris* cells (Du et al., 2012). Thus, cells were grown in BG11 with 1% glucose and cell growth was monitored by optical density (Figure 23) and when cells entered early exponential phase (~0.5 A.U) on day 3, they were harvested, washed in sorbitol mannitol buffer and used immediately for electroporation. Again, RNPs were electroporated into these cells and no auxotrophs were identified. Since the composition of BG11 and BBM are nearly identical, it was deemed unlikely that the growth media was affecting electroporation efficiency.

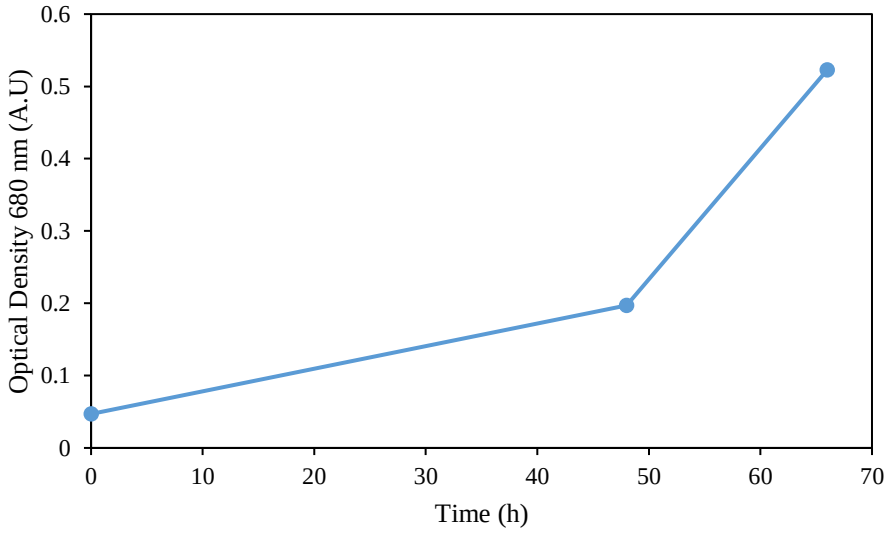

Figure 23 - Growth of *C. vulgaris* in BG11 + 1% glucose media

4.10.2 Monitoring electroporation with cell impermeable probes and flow cytometry

Previous reports have used cell impermeable fluorescent stains to monitor electroporation (Bartoletti et al., 1989). Therefore, cells were electroporated in the presence of Sytox Green (stains dead cells, impermeable to live cells), washed, then stained with propidium iodide (stains dead cells, impermeable to live cells). Afterwards, if counted using flow cytometry, two populations are expected. Cells that were successfully electroporated and alive (green), cells that were electroporated but died or were dead before electroporation (green & red). First, the effect of fixing cells for flow cytometry was evaluated under the microscope (Figure 24). No morphological changes were detected after fixing with either 0.5% v/v or 1.0% v/v formaldehyde and the cell did not aggregate making them amenable to counting with flow cytometry.

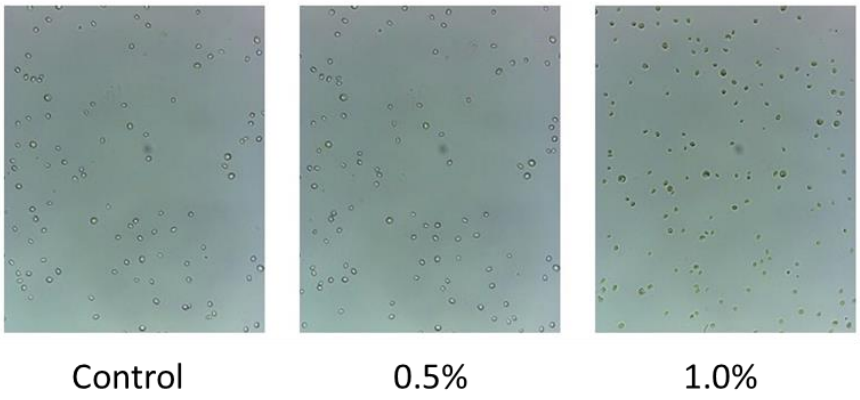

Figure 24 - Effect of formaldehyde concentration on cells.

Secondly, cells were electroporated at 1000 V (square wave, 20 ms) in the presence of PI. As a positive control cells were heat killed and stained with PI, and live cells without stain were used as a negative control. The results indicate that PI was not working as expected as the mean fluorescence of the live and dead control population was the same as seem in Figure 25. PI fluorescence should be higher in the dead cell population.

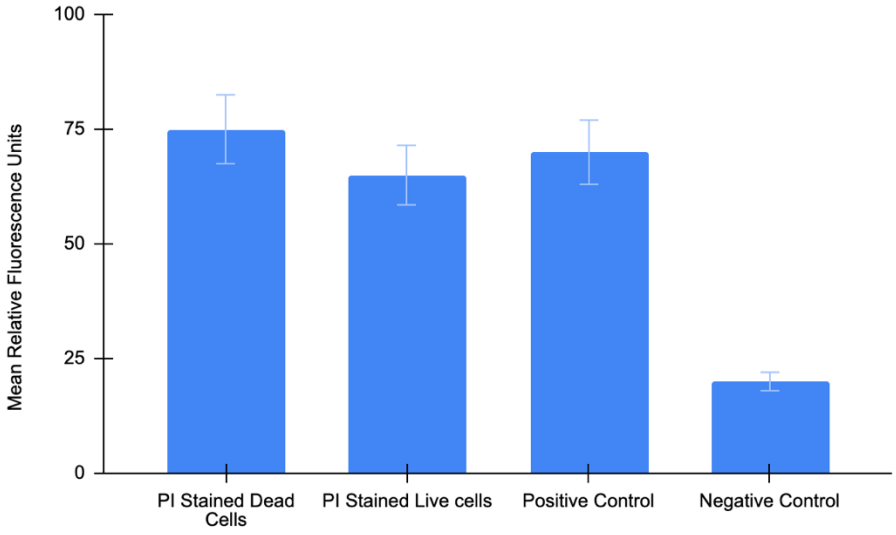

Figure 25 - Mean fluorescence of electroporated cells in the presence of PI (1000 V, square wave, 20 ms).

Since PI was not working as expected, other viability probes were tested. FITC has been reported as a viability stain for microalgae in the literature (Bono et al., 2015). Several electroporation conditions were tested. In this case, a drop in cell viability due to electroporation is expected, however, all the conditions resulted in similar mean fluorescence after electroporation (Figure 26).

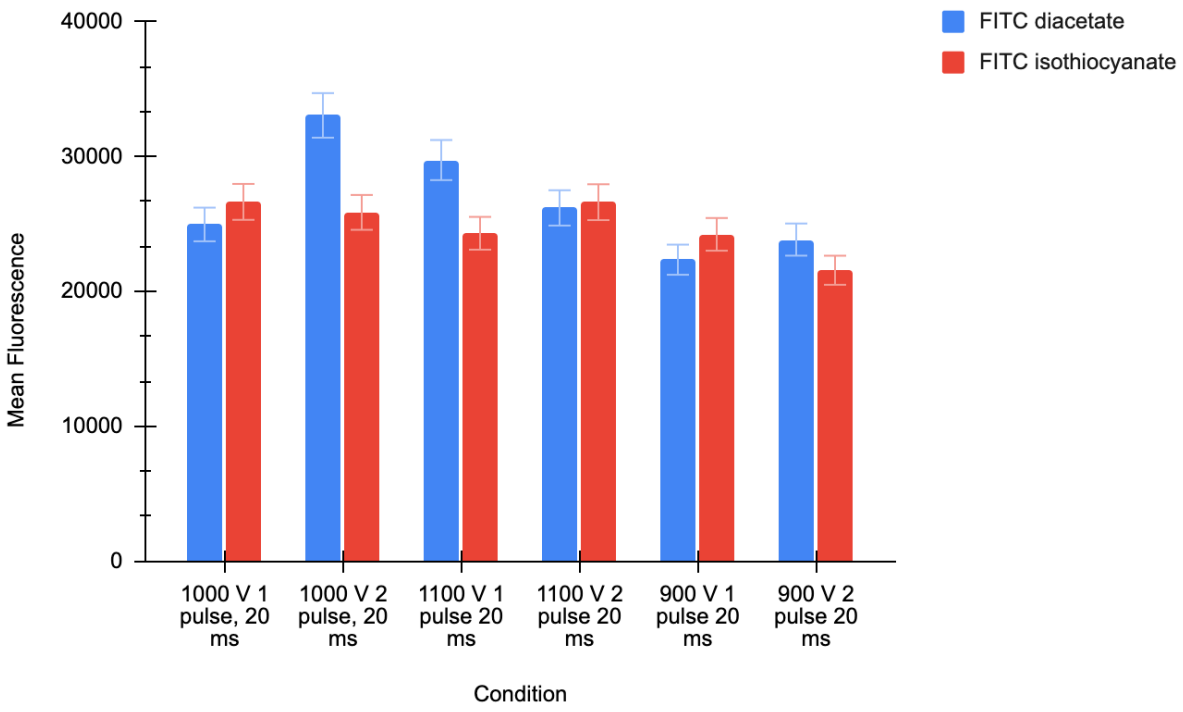

Figure 26 - Mean fluorescence of cells electroporated in the presence of FITC diacetate or FITC isothiocyanate.

It was discovered after the previous flow cytometry experiment that the electroporation boat (device that transfers the electrical impulse to the cuvette containing cells) was not delivering any electrical pulse. Therefore, a new electroporation boat was ordered, and the experiment was repeated. This is the synopsis of the experimental procedure:

FITC: stains live cells

PI: impermeable, stains dead cells

FITC+ PI = cells that were electroporated, survived and up took PI due to temporary increase in cellular permeability.

The data from this experiment was gated to show mean fluorescence for FITC & PI positive cells which is displayed in Figure 27. In this manner, the data is showing the frequency of FITC/PI positive cells in the sample population. As you can see from Figure 27 condition 6 resulted in the highest signal for PI/FITC stained cells. This indicates that 660 V square wave 1 pulse is the most optimum electro for high cell viability and transformation efficiency in *C. vulgaris*.

Conditions:

1. Negative Control
2. Control
3. 1000 V exponential decay wave
4. 1000V, square wave, 2 pulses
5. 660 V, square wave, 2 pulses
6. 660V, square wave, 1 pulse
7. 660V, exponential decay wave,
8. 900V, square wave, 1 pulse
9. 900V, square wave, 2 pulses
10. Control no staining

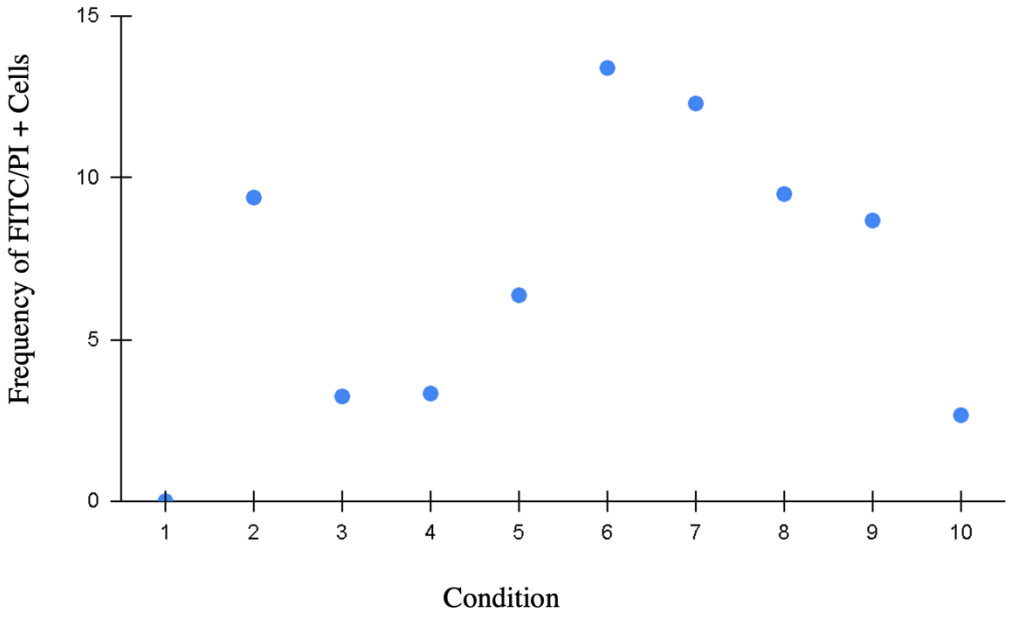

Figure 27 - Flow cytometry FITC/PI + Q2 quadrant data

4.10.3 Effect of protoplasting and PEG mediated transformation of RNPs

As the results of flow cytometry indicated that the stains were not acting as expected in microalgae, electroporation conditions could not be optimized in this manner. Finally, one last attempt to transform *C. vulgaris* using an alternative method was attempted. Protoplasting has been shown to increase the transformation efficiency of plant cells and microalgae (Shillito et al., 1985). First, cells were mixed with a mixture of enzymes capable of degrading the cell wall (lysozyme and sulfatase) at two different cell concentrations. After 16 h incubation period, a sample of the cell was observed under a brightfield microscope Figure 28. There is no quantifiable test for protoplasting, however, cells without a cell wall are expected to aggregate (Maeda et al., 2019).

Compared to the control sample, cells that were protoplasted aggregated in large complexes. Aggregation was more prominent in the lower cell concentration sample (10×10^6 cells/mL) which is not conducive to cell transformation, therefore the higher cell concentration sample was transformed with RNPs using electroporation. However, no auxotrophic colonies appeared following incubation on selective media.

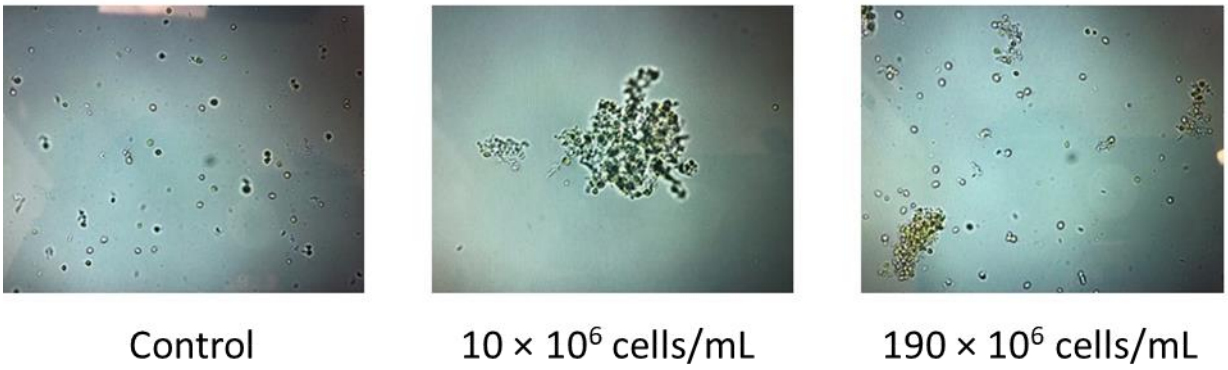

Figure 28 - Comparison of protoplasted cells to untreated control cells under bright field microscope (100 x magnification)

4.11 Conclusions

Delivery of Cas9 RNPs into *C. vulgaris* via electroporation or protoplasting failed to create the expected nitrate auxotrophic strains. Attempts to improve the recovery media and the preparation of competent cells had no effect. Attempts to monitor the electroporation process using fluorescent stains produced confusing results, counter to those expected for these common stains. For example, PI seem to stain cells regardless of cell viability. Since these stains are commonly used in microalgal experiments, it became pertinent to validate the applicability of these stains to counting microalgae cells and determining cell viability.

Chapter 5 – Fluorescent Microscopy

During previous experiments, PI appeared to stain cells regardless of cell viability. In some plants, PI is known to stain pectin containing cell walls (Coskun et al., 2012). As *C. vulgaris* cell walls contains pectin (Gerken et al., 2013), it was hypothesized that PI stains the cell wall of *C. vulgaris* and thus, cell viability cannot be readily determined using this stain. To confirm this hypothesis, several common stains, including PI and a cell wall stain Calcifluor White, were used to stain live and dead cells which were observed under a fluorescent microscope, by flow cytometry, and by fluorometry.

5.1 Determining cellular localization using fluorescent microscopy

First, actively grow (live) microalgae cells were stained with a variety of viability probes as well as Calcifluor White and imaged using fluorescent microscopy. Brightfield images as well as images of each fluorescent channel including chlorophyll autofluorescence were taken and superimposed as can be seen in the following images.

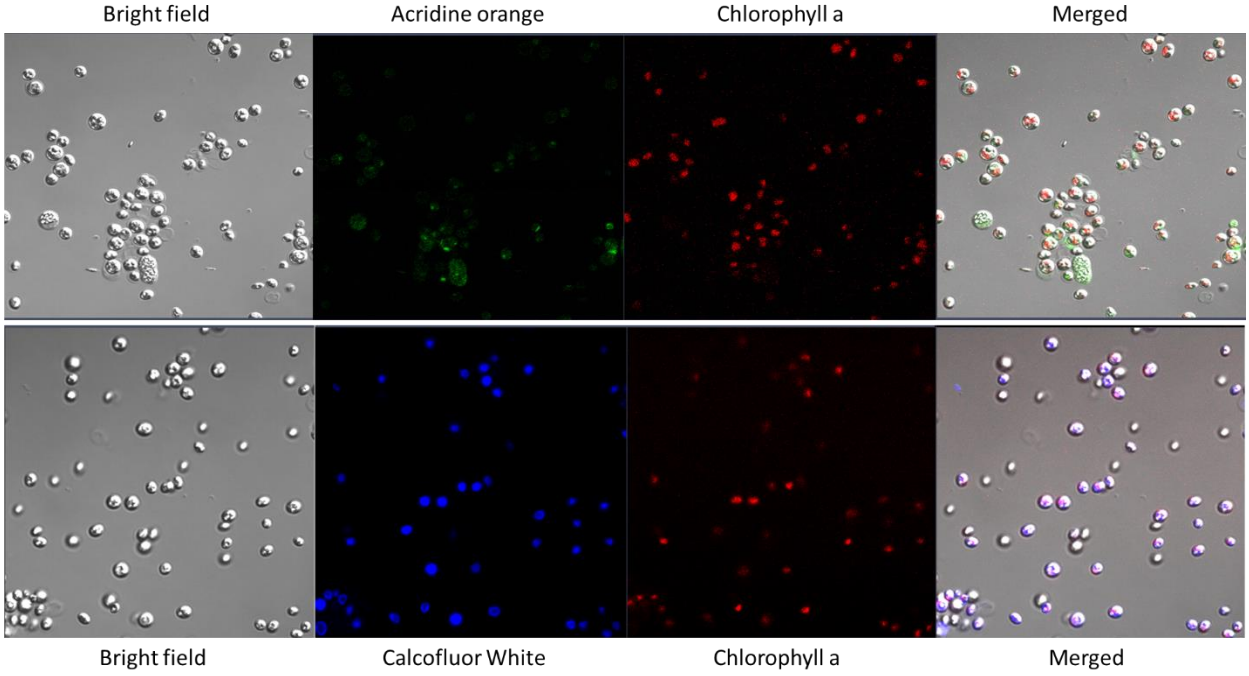

Figure 29 – Visualization of *C. vulgaris* with acridine orange (488/525 nm), Calcofluor White (405/475 nm). Chlorophyll a autofluorescence (372/671 nm) is used for reference. Brightfield and fluorescence channels are merged in the rightmost image.

Acridine orange is a nucleic acid selective dye often used in cell cycle determination. It is cell permeable and as can be seen in Figure 30, fluorescence with acridine orange was rather low, however, the merged

image shows that it is not localized near the chloroplast. As expected, Calcofluor White stains the whole cell since these are intact cells covered in their cell wall (Figure 30). There are several cells that are not stained. This may be due to being slightly out of the plane of focus since several of these cells appear to be partially behind other cells in some cases.

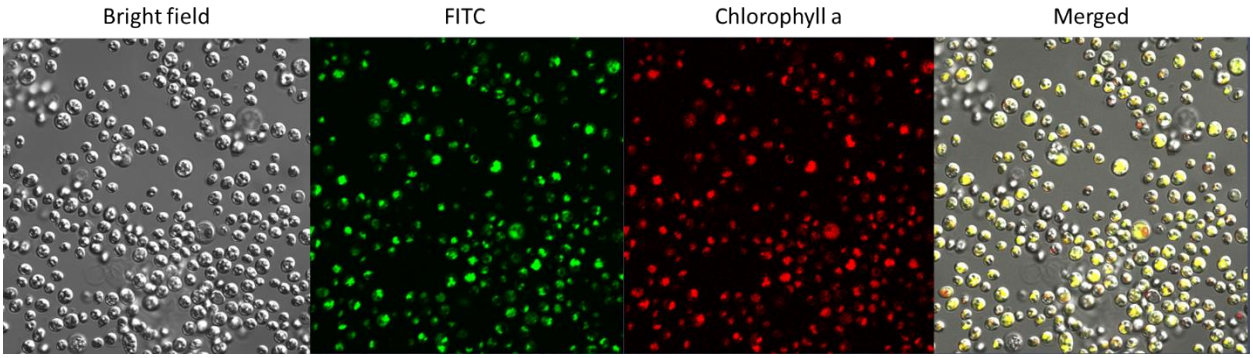

Figure 30 - Visualization of viable cells using FITC (488/520 nm). Chlorophyll a autofluorescence (372/671 nm) is used for reference. Brightfield and fluorescence channels are merged in the rightmost image.

FITC was used to stain live cells and should be permeable to all cells. As can be seen in Figure 31, almost every cell does fluoresce in the FITC channel and gives an almost identical image to cells illuminated by the autofluorescence of chlorophyll. Again, cells out of focus in the top left hand corner do not fluoresce as seen in the Calcofluor White images.

Two stains for dead cells were tested on *C. vulgaris*, Sytox Green and PI. Since live cultures were used, relatively few cells should be stained with these dyes. As can be see in Figure 32, only a few cells are fluorescent when Sytox Green is used, while almost every cell in focus was stained with PI. Since these samples were prepared from the same culture of *C. vulgaris*, this discrepancy is concerning. Furthermore, both of these dyes are nucleic acid stains. It is clear that Sytox is localized to one area of the cell while the PI stains the whole cell. This is more consistent with what was seen when using the cell wall stain, Calcofluor White. Furthermore, Sytox Green had almost no background staining. This is likely because the fluorescence of Sytox Green increases 500 fold upon binding DNA, while PI has low level fluorescence when unbound and when bound to DNA, fluorescence intensity only increase 20 fold (Muñoz et al., 2018).

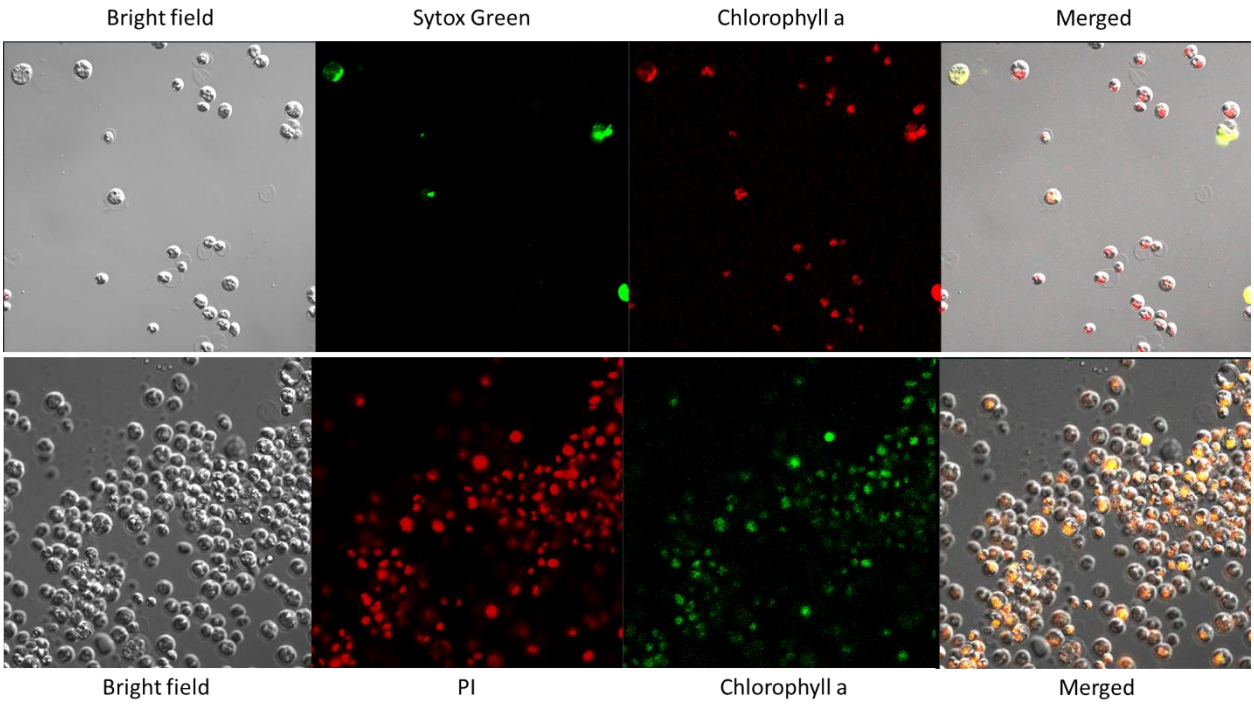

Figure 31 – Visualization of dead cells using Sytox Green (488/525 nm) or PI (488/620 nm). Chlorophyll a autofluorescence (372/671 nm) is used for reference. Brightfield and fluorescence channels are merged in the rightmost image.

5.2 Effect of cell viability on visualization by fluorescent microscopy

To determine whether cell viability affects PI fluorescence, live cells from an actively growing culture were killed using heat (75°C for 20 min). The cell concentration was quantified using a haemocytometer and equal amounts of cells from the live culture and heat killed cells were mixed to obtain the 50% mixture sample. Each sample was stained with PI and imaged (Figure 31).

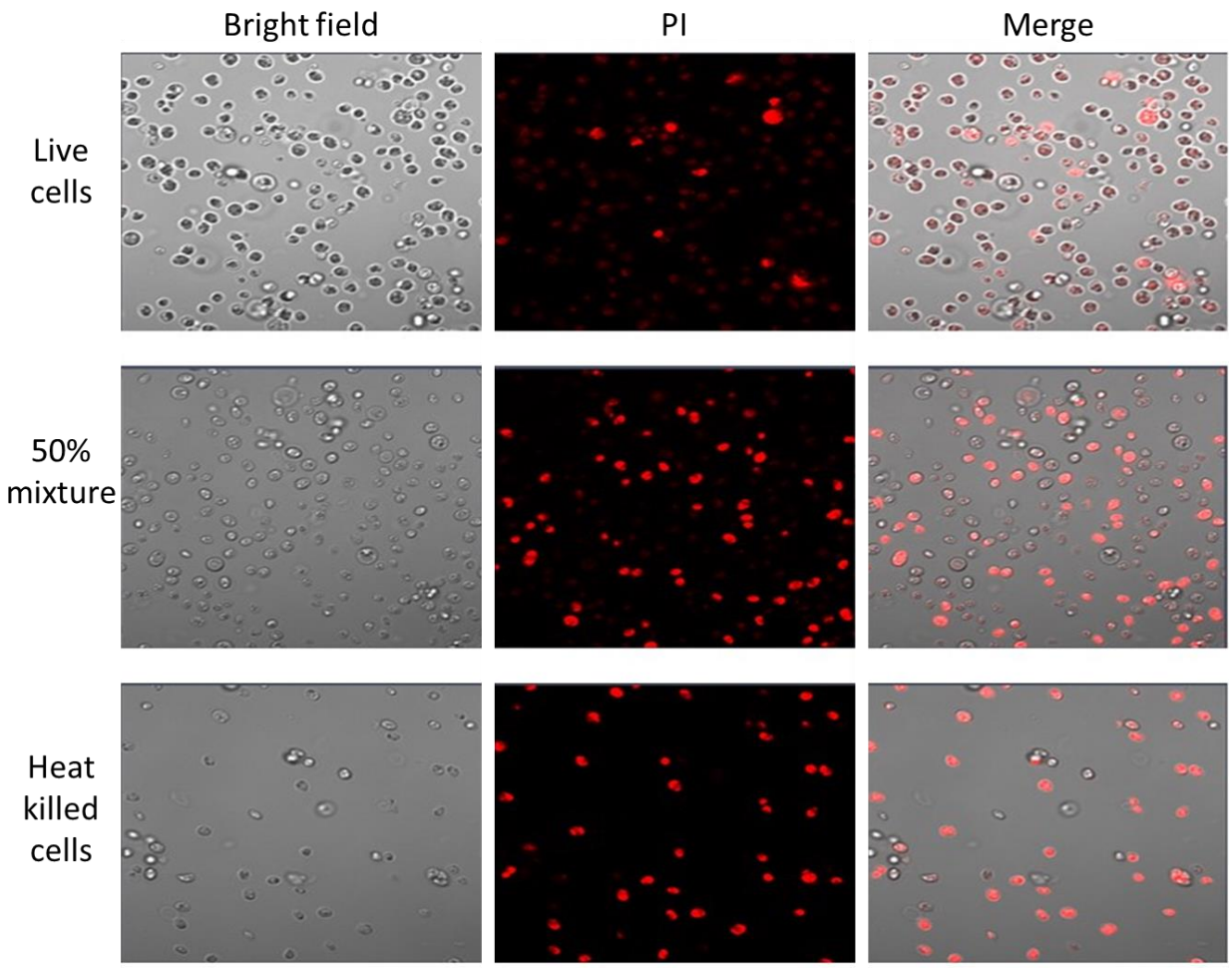

Figure 32 – Effect of cell viability on fluorescence of PI (488/620 nm). The live cells (top panel) were mixed with and equal amount of heat killed cells (bottom panel) to obtain the 50% mixture.

Again, PI can be seen to stain the whole cell and a small number of cells were fluorescing with high intensity in the live culture. A small number of dead cells is expected, however, many of the cells have low level background fluorescence as is seen in the merged image in which nearly every cell is red. This again may be due to cells being out of focus. The dead cells killed using heat were found to still be intact and most exhibited high fluorescence intensity. However, again, many cells were red which may be due to cells out of focus. Since this culture was rendered inviable after heat treatment, nearly all cells should fluoresce. In the mixed sample, the viability was approximately half of the dead cell sample but again there was a high amount of background fluorescence.

5.3 Spectrofluorimetry

Since fluorescence microscopy was inconclusive due to cells being outside of the plane of focus, spectrofluorimetry was used to determine if cell viability and fluorescence intensity were linearly correlated. Again, cells were heat killed as previously described, counted and mixed with an actively growing live culture such that a number of samples with viability between 0-100% were created. These samples were stained with either Sytox Green, PI, or not stained (control) and fluorescence intensity was quantified (Figure 32).

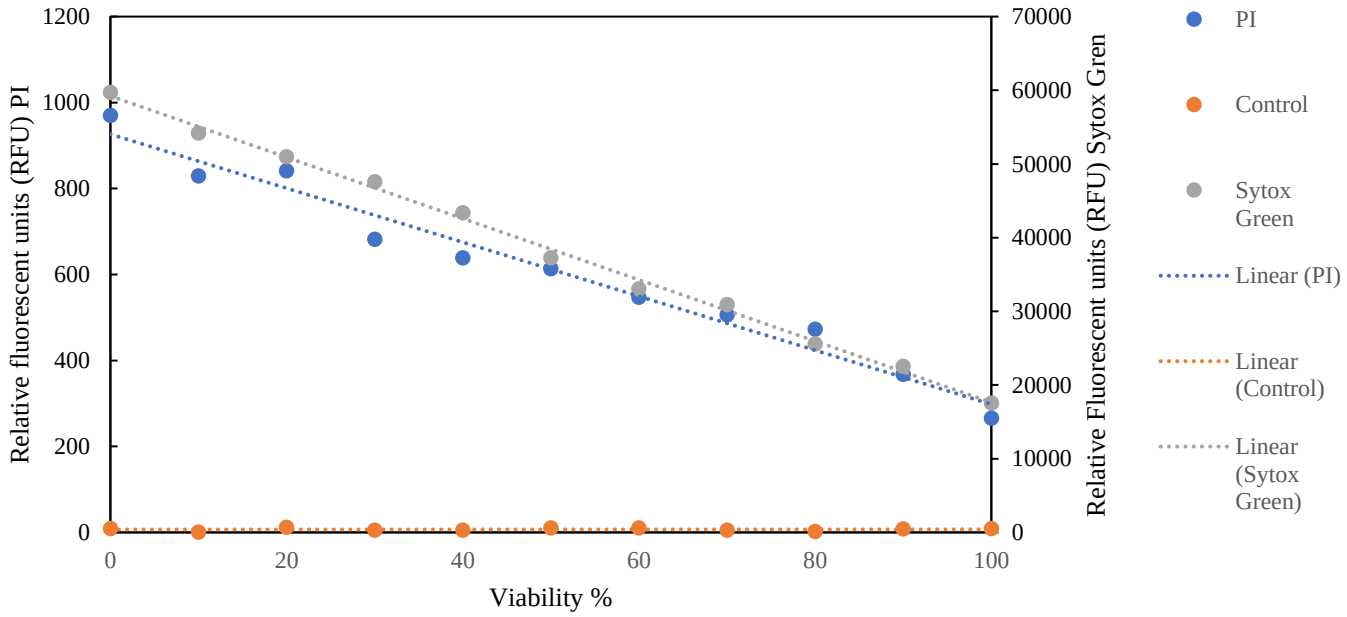

Figure 33 –Relationship between fluorescence intensity of Sytox Green (488/525 nm) and PI (535/617 nm) and cell viability.

The results indicate that both Sytox Green and PI fluorescence increase with decreasing viability of the culture. However, similar to the results from microscopy, PI intensity was much lower than Sytox Green intensity with the viable culture having a fluorescence intensity of 266 ± X RFU versus 17552 ± X RFU respectively. The range of PI intensity (0 versus 100% viable culture) was 704 RFU while the range of Sytox Green was 42150 RFU. This makes Sytox Green a much more robust viability stain for *C. vulgaris*. It should be noted that by using spectrofluorimetry, PI fluorescence intensity could be more accurately measured by using the specific maximum absorption of PI bound to DNA (535 nm), whereas the limited number of lasers available for fluorescence microscopy means that the excitation wavelength used was not optimal (488 nm). This could account for some difference as PI not bound to DNA is preferentially excited

at 493 nm (Muñoz et al., 2018) . However, PI intensity does in fact increase with decreasing viability, the increase was only 3.6-fold over the live culture which limits the utility of this stain. One possible reason for this unexpectedly low increase in fluorescence intensity in *C. vulgaris* may be due to interference by chlorophyll.

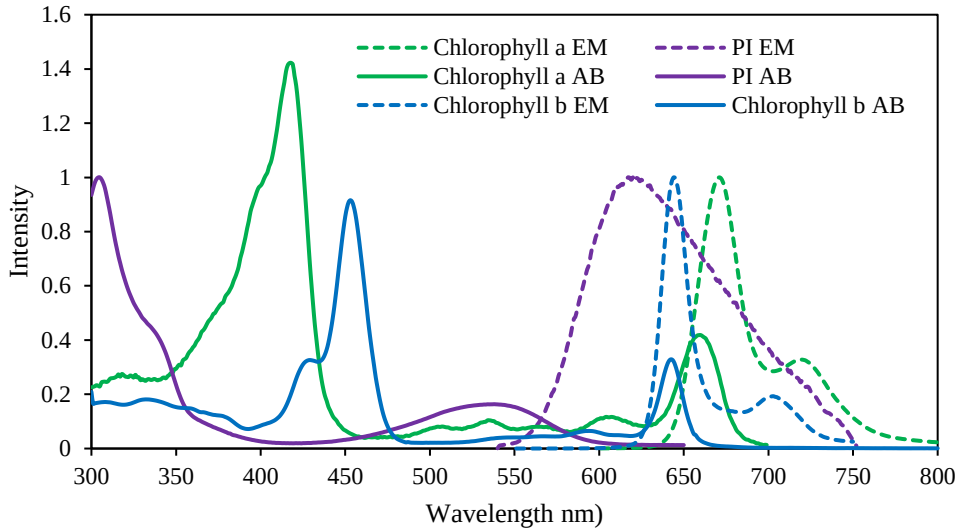

Figure 34 - Fluorescence emission (EM) and absorbance (AB) spectra of PI and chlorophyll a and b. Intensity is normalized to PI absorbance maximum. Data obtained from FPbase (Lambert, 2019).

It is evident from Figure 34 that chlorophyll a and b can both absorb light at 488 nm or 535 nm used to excite PI. They also both exhibit fluorescence in the range or 620 used as the emission wavelength of PI. They also absorb light in this range (620-700 nm). These overlaps are problematic since chlorophyll can potentially absorb the excitation light used as well as the emitted light from PI. Since chlorophyll content of the cells can change significantly depending on cultivation conditions, the interference from chlorophyll will not be consistent. Furthermore, since the response from PI when bound to DNA is rather low, PI is likely a poor choice for measuring viability in chlorophyll containing organisms.

Chapter 6 – Conclusions and Recommendations

Overall, results from the *in vitro* CRISPR-cas9 cleavage assay were inconclusive. Further optimization of this assay to confirm cleavage of the amplified genomic DNA is necessary to be confident that DNA cleavage is happening *in vivo* after electroporation. Use of a selection agent was effective at preventing growth of wild-type C. vulgaris, but no auxotrophic strains were developed. Attempts to monitor the success of electroporation using PI were unsuccessful and it was suspected that PI was staining all cells. This was further confirmed using fluorescence microscopy. While PI fluorescence did increase with decreasing viability, the response was weak, possibly due to chlorophyll interference. Sytox Green was found to be a good viability probe for *C. vulgaris* with low background staining.

Going forward, the success of the sgRNA designs should be confirmed using the *in vitro* cleavage assay. Following that, a liquid selection method may be more successful at generating an auxotroph strain, followed by plating to select for a single clone. Electroporation can be optimized using Sytox Green and FITC which stained cells as expected, rather than PI. Other methods of transformation could also be attempted such as protoplasting followed by PEG/glass bead transformation used for many plant cells.

References

Abidin, A. A. Z., Suntarajh, M., & Yusof, Z. N. B. (2020). Microalgae as a Vaccine Delivery System to Aquatic Organisms. *Microalgae Biotechnology for Food, Health and High Value Products*, 353–372. https://doi.org/10.1007/978-981-15-0169-2_10

Banakar, R., Eggenberger, A. L., Lee, K., Wright, D. A., Murugan, K., Zarecor, S., Lawrence-Dill, C. J., Sashital, D. G., & Wang, K. (2019). High-frequency random DNA insertions upon co-delivery of CRISPR-Cas9 ribonucleoprotein and selectable marker plasmid in rice. *Scientific Reports 2019 9:1*, *9*(1), 1–13. https://doi.org/10.1038/s41598-019-55681-y

Bartoletti, D. C., Harrison, G. I., & Weaver, J. C. (1989). The number of molecules taken up by electroporated cells: quantitative determination. FEBS Letters, 256(1–2), 4–10. https://doi.org/10.1016/0014-5793(89)81707-7

Bono, M. S., Garcia, R. D., Sri-Jayantha, D. V., Ahner, B. A., & Kirby, B. J. (2015). Measurement of lipid accumulation in Chlorella vulgaris via flow cytometry and liquid-state 1H NMR spectroscopy for development of an NMR-traceable flow cytometry protocol. *PLoS ONE*, *10*(8), e0134846. https://doi.org/10.1371/journal.pone.0134846

Butt, H., Eid, A., Ali, Z., Atia, M. A. M., Mokhtar, M. M., Hassan, N., Lee, C. M., Bao, G., & Mahfouz, M. M. (2017). Efficient CRISPR/Cas9-Mediated Genome Editing Using a Chimeric Single-Guide RNA Molecule. *Frontiers in Plant Science*, *0*, 1441. https://doi.org/10.3389/FPLS.2017.01441

Cecchin, M., Marcolungo, L., Rossato, M., Girolomoni, L., Cosentino, E., Cuine, S., Li-Beisson, Y., Delledonne, M., & Ballottari, M. (2019). Chlorella vulgaris genome assembly and annotation reveals the molecular basis for metabolic acclimation to high light conditions. *The Plant Journal*, *100*(6), 1289–1305. https://doi.org/10.1111/TPJ.14508

Coelho, D., Lopes, P. A., Cardoso, V., Ponte, P., Brás, J., Madeira, M. S., Alfaia, C. M., Bandarra, N. M., Gerken, H. G., Fontes, C. M. G. A., & Prates, J. A. M. (2019). Novel combination of feed enzymes to improve the degradation of Chlorella vulgaris recalcitrant cell wall. *Scientific Reports*, *9*(1), 1–11. https://doi.org/10.1038/s41598-019-41775-0

Coskun, D., Britto, D. T., Jean, Y.-K., Schulze, L. M., Becker, A., & Kronzucker, H. J. (2012). Silver ions disrupt K+ homeostasis and cellular integrity in intact barley (Hordeum vulgare L.) roots. *Journal of Experimental Botany*, *63*(1), 151–162. https://doi.org/10.1093/JXB/ERR267

Dawson, H. N., Pendleton, L. C., Solomonson, L. P., & Cannons, A. C. (1996). Cloning and characterization of the nitrate reductase-encoding gene from Chlorella vulgaris: structure and identification of transcription start points and initiator sequences. *Gene*, *171*(2), 139–145. https://doi.org/10.1016/0378-1119(96)00063-7

De Morais, M. G., Vaz, B. D. S., De Morais, E. G., & Costa, J. A. V. (2015). Biologically Active Metabolites Synthesized by Microalgae. *BioMed Research International*, *2015*. https://doi.org/10.1155/2015/835761

Doron, L., Segal, N., & Shapira, M. (2016). Transgene Expression in Microalgae—From Tools to Applications. *Frontiers in Plant Science*, *0*(APR2016), 505. https://doi.org/10.3389/FPLS.2016.00505

Doudna, J. A., & Charpentier, E. (2014). The new frontier of genome engineering with CRISPR-Cas9. *Science*, *346*(6213). https://doi.org/10.1126/SCIENCE.1258096

Du, Z., Hu, B., Shi, A., Ma, X., Cheng, Y., Chen, P., Liu, Y., Lin, X., & Ruan, R. (2012). Cultivation of a microalga Chlorella vulgaris using recycled aqueous phase nutrients from hydrothermal carbonization process. *Bioresource Technology*, *126*, 354–357. https://doi.org/10.1016/J.BIORTECH.2012.09.062

Du, Z., Hu, B., Shi, A., Ma, X., Cheng, Y., Chen, P., Liu, Y., Lin, X., & Ruan, R. (2012). Cultivation of a microalga Chlorella vulgaris using recycled aqueous phase nutrients from hydrothermal carbonization process. Bioresource Technology, 126, 354–357. https://doi.org/10.1016/J.BIORTECH.2012.09.062

Fan, J., Ning, K., Zeng, X., Luo, Y., Wang, D., Hu, J., Li, J., Xu, H., Huang, J., Wan, M., Wang, W., Zhang, D., Shen, G., Run, C., Liao, J., Fang, L., Huang, S., Jing, X., Su, X., … Li, Y. (2015). Genomic Foundation of Starch-to-Lipid Switch in Oleaginous Chlorella spp. *Plant Physiology*, *169*(4), 2444. https://doi.org/10.1104/PP.15.01174

Gaj, T., Gersbach, C. A., & Barbas, C. F. (2013). ZFN, TALEN, and CRISPR/Cas-based methods for genome engineering. *Trends in Biotechnology*, *31*(7), 397–405. https://doi.org/10.1016/J.TIBTECH.2013.04.004

Gouveia, L., Rema, P., Pereira, O., & Empis, J. (2003). Colouring ornamental fish (Cyprinus carpio and Carassius auratus) with microalgal biomass. *Aquaculture Nutrition*, *9*(2), 123–129. https://doi.org/10.1046/J.1365-2095.2003.00233.X

Guedes, A. C., Amaro, H. M., & Malcata, F. X. (2011). Microalgae as Sources of Carotenoids. *Marine*

Drugs, *9*(4), 625. https://doi.org/10.3390/MD9040625

Gupta, R. M., & Musunuru, K. (2014). Expanding the genetic editing tool kit: ZFNs, TALENs, and CRISPR-Cas9. *The Journal of Clinical Investigation*, *124*(10), 4154–4161. https://doi.org/10.1172/JCI72992

Higashiyama, T., Maki, S., & Yamada, T. (1995). Molecular organization of Chlorella vulgaris chromosome I: presence of telomeric repeats that are conserved in higher plants. *Mgg Molecular & General Genetics*, *246*(1), 29–36. https://doi.org/10.1007/BF00290130

Hu, Q., Sommerfeld, M., Jarvis, E., Ghirardi, M., Posewitz, M., Seibert, M., & Darzins, A. (2008). Microalgal triacylglycerols as feedstocks for biofuel production: perspectives and advances. *The Plant Journal*, *54*(4), 621–639. https://doi.org/10.1111/J.1365-313X.2008.03492.X

Huarachi-Olivera, R., Dueñas-Gonza, A., Yapo-Pari, U., Vega, P., Romero-Ugarte, M., Tapia, J., Molina, L., Lazarte-Rivera, A., Pacheco-Salazar, D. G., & Esparza, M. (2018). Bioelectrogenesis with microbial fuel cells (MFCs) using the microalga Chlorella vulgaris and bacterial communities. *Electronic Journal of Biotechnology*, *31*, 34–43. https://doi.org/10.1016/j.ejbt.2017.10.013

Imamoglu, E., Dalay, M. C., & Sukan, F. V. (2009). Influences of different stress media and high light intensities on accumulation of astaxanthin in the green alga Haematococcus pluvialis. *New Biotechnology*, *26*(3–4), 199–204. https://doi.org/10.1016/J.NBT.2009.08.007

Jeon, S., Lim, J. M., Lee, H. G., Shin, S. E., Kang, N. K., Park, Y. Il, Oh, H. M., Jeong, W. J., Jeong, B. R., & Chang, Y. K. (2017). Current status and perspectives of genome editing technology for microalgae. In *Biotechnology for Biofuels* (Vol. 10, Issue 1, p. 267). BioMed Central Ltd. https://doi.org/10.1186/s13068-017-0957-z

Ji, L., & Fan, J. (2020a). Electroporation Procedures for Genetic Modification of Green Algae (<Emphasis Type="Italic">Chlorella</Emphasis> spp.). *Methods in Molecular Biology*, *2050*, 181–185. https://doi.org/10.1007/978-1-4939-9740-4_20

Ji, L., & Fan, J. (2020b). Electroporation Procedures for Genetic Modification of Green Algae (Chlorella spp.). In *Methods in Molecular Biology* (Vol. 2050, pp. 181–185). Humana Press Inc. https://doi.org/10.1007/978-1-4939-9740-4_20

Jung, B., Sivasubramanian, • R, Batchelor, • B, & Abdel-Wahab, • A. (n.d.). Chlorate reduction by dithionite/UV advanced reduction process. https://doi.org/10.1007/s13762-016-1132-y

Kawasaki, K., & Kamagata, Y. (2017). Phosphate-catalyzed hydrogen peroxide formation from agar,

gellan, and κ-carrageenan and recovery of microbial cultivability via catalase and pyruvate. Applied and Environmental Microbiology, 83(21). https://doi.org/10.1128/AEM.01366-17

Khoeyi, Z. A., Seyfabadi, J., & Ramezanpour, Z. (2011). Effect of light intensity and photoperiod on biomass and fatty acid composition of the microalgae, Chlorella vulgaris. *Aquaculture International 2011 20:1*, *20*(1), 41–49. https://doi.org/10.1007/S10499-011-9440-1

Kilian, O., Benemann, C. S. E., Niyogi, K. K., & Vick, B. (2011). High-efficiency homologous recombination in the oil-producing alga Nannochloropsis sp. *Proceedings of the National Academy of Sciences*, *108*(52), 21265–21269. https://doi.org/10.1073/PNAS.1105861108

Kim, J., Chang, K. S., Lee, S., & Jin, E. (2021). Establishment of a Genome Editing Tool Using CRISPR-Cas9 in Chlorella vulgaris UTEX395. *International Journal of Molecular Sciences 2021, Vol. 22, Page 480*, *22*(2), 480. https://doi.org/10.3390/IJMS22020480

Kindle, K. L., Richards, K. L., & Stern, D. B. (1991). Engineering the chloroplast genome: techniques and capabilities for chloroplast transformation in Chlamydomonas reinhardtii. *Proceedings of the National Academy of Sciences*, *88*(5), 1721–1725. https://doi.org/10.1073/PNAS.88.5.1721

Kong, W., Song, H., Cao, Y., Yang, H., Hua, S., & Xia, C. (2013). The characteristics of biomass production, lipid accumulation and chlorophyll biosynthesis of *Chlorella vulgaris* under mixotrophic cultivation. *African Journal of Biotechnology*, *10*(55), 11620–11630. https://doi.org/10.4314/ajb.v10i55.

Kumar, A., Ergas, S., Yuan, X., Sahu, A., Zhang, Q., Dewulf, J., Malcata, F. X., & van Langenhove, H. (2010). Enhanced CO2 fixation and biofuel production via microalgae: recent developments and future directions. *Trends in Biotechnology*, *28*(7), 371–380. https://doi.org/10.1016/J.TIBTECH.2010.04.004

Kumar, M., Jeon, J., Choi, J., & Kim, S. R. (2018a). Rapid and efficient genetic transformation of the green microalga Chlorella vulgaris. *Journal of Applied Phycology*, *30*(3), 1735–1745. https://doi.org/10.1007/s10811-018-1396-3

Kumar, M., Jeon, J., Choi, J., & Kim, S. R. (2018b). Rapid and efficient genetic transformation of the green microalga Chlorella vulgaris. *Journal of Applied Phycology*, *30*(3), 1735–1745. https://doi.org/10.1007/s10811-018-1396-3

Lambert, TJ (2019) FPbase: a community-editable fluorescent protein database. Nature Methods. 16, 277–278. doi: 10.1038/s41592-019-0352-8

Lau, C. C., Loh, S. H., Aziz, A., & Cha, T. S. (2017). Effects of disrupted omega-3 desaturase gene

construct on fatty acid composition and expression of four fatty acid biosynthetic genes in transgenic Chlorella vulgaris. *Algal Research*, *26*, 143–152. https://doi.org/10.1016/J.ALGAL.2017.07.011

León-Bañares, R., González-Ballester, D., Galván, A., & Fernández, E. (2004). Transgenic microalgae as green cell-factories. *Trends in Biotechnology*, *22*(1), 45–52. https://doi.org/10.1016/J.TIBTECH.2003.11.003

Li, D.-W., Balamurugan, S., Zheng, J.-W., Yang, W.-D., Liu, J.-S., & Li, H.-Y. (2020). Rapid and Effective Electroporation Protocol for <Emphasis Type="Italic">Nannochloropsis oceanica</Emphasis>. *Methods in Molecular Biology*, *2050*, 175–179. https://doi.org/10.1007/978-1-4939-9740-4_19

Lin, H. Di, Liu, B. H., Kuo, T. T., Tsai, H. C., Feng, T. Y., Huang, C. C., & Chien, L. F. (2013). Knockdown of PsbO leads to induction of HydA and production of photobiological H2 in the green alga Chlorella sp. DT. *Bioresource Technology*, *143*, 154–162. https://doi.org/10.1016/J.BIORTECH.2013.05.101

Maeda, K., Kunieda, T., Tamura, K., Hatano, K., Hara-Nishimura, I., & Shimada, T. (2019). Identification of Periplasmic Root-Cap Mucilage in Developing Columella Cells of Arabidopsis thaliana. Plant and Cell Physiology, 60(6), 1296–1303. https://doi.org/10.1093/PCP/PCZ047

Mata, T. M., Martins, A. A., & Caetano, N. S. (2010). Microalgae for biodiesel production and other applications: A review. *Renewable and Sustainable Energy Reviews*, *14*(1), 217–232. https://doi.org/10.1016/J.RSER.2009.07.020

Mujtaba, G., Choi, W., Lee, C. G., & Lee, K. (2012). Lipid production by Chlorella vulgaris after a shift from nutrient-rich to nitrogen starvation conditions. *Bioresource Technology*, *123*, 279–283. https://doi.org/10.1016/J.BIORTECH.2012.07.057

Muñoz, C. F., de Jaeger, L., Sturme, M. H. J., Lip, K. Y. F., Olijslager, J. W. J., Springer, J., Wolbert, E. J. H., Martens, D. E., Eggink, G., Weusthuis, R. A., & Wijffels, R. H. (2018). Improved DNA/protein delivery in microalgae – A simple and reliable method for the prediction of optimal electroporation settings. *Algal Research*, *33*, 448–455. https://doi.org/10.1016/j.algal.2018.06.021

Nymark, M., Sharma, A. K., Sparstad, T., Bones, A. M., & Winge, P. (2016). A CRISPR/Cas9 system adapted for gene editing in marine algae. *Scientific Reports 2016 6:1*, *6*(1), 1–6. https://doi.org/10.1038/srep24951

Orr, V., & Rehmann, L. (2014). Improvement of the Nile Red fluorescence assay for determination of

total lipid content in microalgae independent of chlorophyll content. *Journal of Applied Phycology 2014 27:6*, *27*(6), 2181–2189. https://doi.org/10.1007/S10811-014-0481-5

Orr, V., & Rehmann, L. (2015). Improvement of the Nile Red fluorescence assay for determination of total lipid content in microalgae independent of chlorophyll content. *Journal of Applied Phycology*, *27*(6), 2181–2189. https://doi.org/10.1007/s10811-014-0481-5

Panahi, Y., Khosroshahi, A. Y., Sahebkar, A., & Heidari, H. R. (2019). Impact of cultivation condition and media content on Chlorella vulgaris composition. In *Advanced Pharmaceutical Bulletin* (Vol. 9, Issue 2, pp. 182–194). Tabriz University of Medical Sciences. https://doi.org/10.15171/apb.2019.022

Poliner, E. (2017). *CHARACTERIZATION OF NANNOCHLOROPSIS OCEANICA CCMP1779 GROWN IN LIGHT:DARK CYCLES INFORMS GENETIC ENGINEERING TOOL DEVELOPMENT*.

Ru, I. T. K., Sung, Y. Y., Jusoh, M., Wahid, M. E. A., & Nagappan, T. (2020). Chlorella vulgaris: a perspective on its potential for combining high biomass with high value bioproducts. *Applied Phycology*, *1*(1), 2–11. https://doi.org/10.1080/26388081.2020.1715256

Run, C., Fang, L., Fan, J., Fan, C., Luo, Y., Hu, Z., & Li, Y. (2016). Stable nuclear transformation of the industrial alga Chlorella pyrenoidosa. *Algal Research*, *17*, 196–201. https://doi.org/10.1016/J.ALGAL.2016.05.002

Safi, C., Zebib, B., Merah, O., Pontalier, P. Y., & Vaca-Garcia, C. (2014). Morphology, composition, production, processing and applications of Chlorella vulgaris: A review. *Renewable and Sustainable Energy Reviews*, *35*, 265–278. https://doi.org/10.1016/J.RSER.2014.04.007

Sanford, J. C. (1990). Biolistic plant transformation. *Physiologia Plantarum*, *79*(1), 206–209. https://doi.org/10.1111/J.1399-3054.1990.TB05888.X

Seki, A., & Rutz, S. (2018). Optimized RNP transfection for highly efficient CRISPR/Cas9-mediated gene knockout in primary T cells. *Journal of Experimental Medicine*, *215*(3), 985–997. https://doi.org/10.1084/JEM.20171626

Slattery, S., A, D., H, W., JA, T., JT, L., T, J., K, L., Z, K., I, D.-P., BJ, K., & DR, E. (2018). An Expanded Plasmid-Based Genetic Toolbox Enables Cas9 Genome Editing and Stable Maintenance of Synthetic Pathways in Phaeodactylum tricornutum. *ACS Synthetic Biology*, *7*(2), 328–338. https://doi.org/10.1021/ACSSYNBIO.7B00191

Solomonson, L. P., & McCreery, M. J. (1986). Radiation inactivation of assimilatory NADH:nitrate reductase from Chlorella. Catalytic and physical sizes of functional units. *Journal of Biological*

Chemistry, *261*(2), 806–810. https://doi.org/10.1016/S0021-9258(17)36167-7

Specht, E., Miyake-Stoner, S., & Mayfield, S. (2010). Micro-algae come of age as a platform for recombinant protein production. *Biotechnology Letters 2010 32:10*, *32*(10), 1373–1383. https://doi.org/10.1007/S10529-010-0326-5

Spolaore, P., Joannis-Cassan, C., Duran, E., & Isambert, A. (2006). Commercial applications of microalgae. *Journal of Bioscience and Bioengineering*, *101*(2), 87–96. https://doi.org/10.1263/JBB.101.87

Stein, J. (1973). *Handbook of Phycological Methods: Culture Methods and Growth Measurements - Google Books*. https://books.google.ca/books?hl=en&lr=&id=yJw8AAAAIAAJ&oi=fnd&pg=PR11&dq=Stein,+J.+(ED.)+Handbook+of+Phycological+methods.+Culture+methods+and+growth+measurements.+Cambridge+University+Press.+448+pp.&ots=l62Cm6AkPb&sig=RqHTM33YprmDO5_-Vc1qXh_-k04#v=onepa

Takahashi, T. (2019). Routine Management of Microalgae Using Autofluorescence from Chlorophyll. *Molecules*, *24*(24). https://doi.org/10.3390/MOLECULES24244441

Tang, Z., Chen, S., Chen, A., He, B., Zhou, Y., Chai, G., Guo, F., & Huang, J. (2019). CasPDB: an integrated and annotated database for Cas proteins from bacteria and archaea. *Database*, *2019*(1), 93. https://doi.org/10.1093/DATABASE/BAZ093

Vidal, L., Pinsach, J., Striedner, G., Caminal, G., & Ferrer, P. (2008). Development of an antibiotic-free plasmid selection system based on glycine auxotrophy for recombinant protein overproduction in Escherichia coli. *Journal of Biotechnology*, *134*(1–2), 127–136. https://doi.org/10.1016/J.JBIOTEC.2008.01.011

Vos, M., & Didelot, X. (2008). A comparison of homologous recombination rates in bacteria and archaea. *The ISME Journal 2009 3:2*, *3*(2), 199–208. https://doi.org/10.1038/ismej.2008.93

Widjaja, A., Chien, C. C., & Ju, Y. H. (2009). Study of increasing lipid production from fresh water microalgae Chlorella vulgaris. *Journal of the Taiwan Institute of Chemical Engineers*, *40*(1), 13–20. https://doi.org/10.1016/j.jtice.2008.07.007

Wright, O., Delmans, M., Stan, G.-B., & Ellis, T. (2014). GeneGuard: A Modular Plasmid System Designed for Biosafety. *ACS Synthetic Biology*, *4*(3), 307–316. https://doi.org/10.1021/SB500234S

Yang, B., Liu, J., Liu, B., Sun, P., Ma, X., Jiang, Y., Wei, D., & Chen, F. (2015). Development of a stable genetic system for Chlorella vulgaris-A promising green alga for CO2 biomitigation. *Algal*

Research, *12*, 134–141. https://doi.org/10.1016/j.algal.2015.08.012

Zhang, Y. T., Jiang, J. Y., Shi, T. Q., Sun, X. M., Zhao, Q. Y., Huang, H., & Ren, L. J. (2019). Application of the CRISPR/Cas system for genome editing in microalgae. In *Applied Microbiology and Biotechnology* (Vol. 103, Issue 8, pp. 3239–3248). Springer Verlag. https://doi.org/10.1007/s00253-019-09726-x

Zhang, Z., Wan, T., Chen, Y., Chen, Y., Sun, H., Cao, T., Songyang, Z., Tang, G., Wu, C., Ping, Y., Xu, F.-J., & Huang, J. (2019). Cationic Polymer-Mediated CRISPR/Cas9 Plasmid Delivery for Genome Editing. *Macromolecular Rapid Communications*, *40*(5), 1800068. https://doi.org/10.1002/MARC.201800068

Appendix A – Primer table

Table 15 - Primers used in this work

Name	Sequence
1-F NR PCR Primer	CAGGCGATACATACTTGGTTATGC
1-R NR PCR Primer	CTTCTCAATCAGCTTGAACGACTG
2-F NR PCR Primer	TTGGTGAGTGAGAGTGTAACTAGC
2-R NR PCR Primer	GATAGCAGCAGTTGTTCATCATCC
3-F NR PCR Primer	CTCCTCATTCATTTCATCTCTCACCTTTC
3-R NR PCR Primer	TGGTCAAGGATGCATAACCAAGTATGTA
gRNA1_F	GGAGGCAGCAGCACCAGCGCGTTTTAGAGCTAGAAATAGCAAG
tracrRNA_rev	AATTACATTCAAAGAACATGTGAG CAA AAG
T7 Promoter_fwd	CATGTTCTTTGAATGTAATTCAGCTCCG
gRNA1_R	GCGCTGGTGCTGCTGCCTCCCCTATAGTGAGTCGTATTAATT TC
gRNA2(1)_F	GCAGGCAGCCAATTGCCGCAGTTTTAGAGCTAGAAATAGCAAG
gRNA2(1)_R	TGCGGCAATTGGCTGCCTGCCCTATAGTGAGTCGTATTAATTTC
gRNA2(2)_F	GGCGCGGCAGCAAGCAGGCGGTTTTAGAGCTAGAAATAGCAAG
gRNA2(2)_R	CGCCTGCTTGCTGCCGCGCCCCTATAGTGAGTCGTATTAATTTC
gRNA_3_F	GGCAGCAGCACTTTCAGCAGGTTTTAGAGCTAGAAATAGCAAG
gRNA_3_R	CTGCTGAAAGTGCTGCTGCCCCTATAGTGAGTCGTATTAATTTC
cPCR_T7_F	CATCATTCCGTGGCGTTATCC
cCPR_gRNA	GAGAGTCAATTCAGGGTGGT
seq_petT7	ATACCCACGCCGAAACAAGC
T7pT_F	GCGACTCCTGCATTAGG
T7pT_R	AAAGCACCGACTCGGTG
eGFP_F	GCCTCTTCGCTATTACGCCA
eGFP_R	TCATGTTTGACAGCTTATCATCGG
HR_1F_fwd	CTTGCATGCCTCACCAGTCACGCCGCTTC
HR_1F_rev	TCGACCTGCACTGGTGCTGCTGCCTCCT
eGFP_fwd	GCAGCACCAGTGCAGGTCGATCTAGAGG
eGFP_rev	CCGCTGGCGCTCATCGGATCTAGTAACATAGATG
HR_1R_fwd	GATCCGATGAGCGCCAGCGGCGGCAATC
HR_1R_rev	TGACAGCTTATAAGTGGGATACCAGCTATGCATTCAAATCCGAGC

eGFP BB_fwd	ATCCCACTTATAAGCTGTCAAACATGAGAATTCGTAATC
eGFP BB_rev	TGACTGGTGAGGCATGCAAGCTTGGCAC
HR_1Fb_fwd	CTTGCATGCCCGTTGCCGGCTCAGTGTATAAC
HR_1Fb_rev	TCGACCTGCAGCACGGAGTGTCGCAGGC
eGFPb_fwd	CACTCCGTGCTGCAGGTCGATCTAGAGG
eGFPb_rev	GCCAATTGCCTCATCGGATCTAGTAACATAGATG
HR_1Rb_fwd	GATCCGATGAGGCAATTGGCTGCCTGCC
HR_1Rb_rev	TGACAGCTTATTGGCTTTGAGCGAGTGGATG
eGFPb BB_fwd	TCAAAGCCAATAAGCTGTCAAACATGAGAATTCGTAATC
eGFPb BB_rev	GCCGGCAACGGGCATGCAAGCTTGGCAC
HR_1Fc_fwd	CTTGCATGCCAACTCCGAAGGTGGGCGC
HR_1Fc_rev	TCGACCTGCACCTCAGCGCCCAGGTGAG
eGFPc_fwd	GGCGCTGAGGTGCAGGTCGATCTAGAGG
eGFPc_rev	CAGCAAGCAGTCATCGGATCTAGTAACATAGATG
HR_1Rc_fwd	GATCCGATGACTGCTTGCTGCCGCGCCT
HR_1Rc_rev	TGACAGCTTAGTATCGCCTGTCACTTTGCGGG
eGFPc BB_fwd	CAGGCGATACTAAGCTGTCAAACATGAGAATTCGTAATC
eGFPc BB_rev	CTTCGGAGTTGGCATGCAAGCTTGGCAC
HR_1Fd_fwd	CTTGCATGCCGGAGCTTGGAGGTGCCCATTG
HR_1Fd_rev	TCGACCTGCACAGCGGCAGAGGGCAGGA
eGFPd_fwd	TCTGCCGCTGTGCAGGTCGATCTAGAGG
eGFPd_rev	GCACTTTCAGTCATCGGATCTAGTAACATAGATG
HR_1Rd_fwd	GATCCGATGACTGAAAGTGCTGCTGCCG
HR_1Rd_rev	TGACAGCTTACACTTGGCATAAAGGAAGACG
eGFPd BB_fwd	ATGCCAAGTGTAAGCTGTCAAACATGAGAATTCGTAATC
eGFPd BB_rev	TCCAAGCTCCGGCATGCAAGCTTGGCAC
eGFP_SEQ	GCTGCAAGGCGATTAAGTTGG
cPCR	TGTTTGAACGATCTGCAGCC
500_F1	CCAACCTGATGCTGCTGAAC
500_R1	ACACAGCAGCGCCAGCAG
1000_F1	GCCGCTTCTGTTCTGTTTCCAC
1000_R1	ATGCATAGCTGGTATCCCACTTA
500_F2	CTGTGACGCACGAGGGGCAAC

500_R2	TCCTAGTTGTTGCAGCACGCC
1000_F2	CGTTGCCGGCTCAGTGTATAA
1000_R2	CCATCCACTCGCTCAAAGCCAA
500_F3	CCGCCCGGGTGCCGCACA
500_R3	AGCACCCCACCATTGCC
1000_F3	AACTCCGAAGGTGGGCGC
1000_R3	AGCCATTGCTGTTTTTGTTGACAC
500_F4	TGCCAGCCGCACGGCACTTT
500_R4	AGAAGCAGCTGCTGGAGTACTACATTGG
1000_F4	GGAGCTTGGAGGTGCCCATTGGT
1000_R4	AAGCACGTCTTCCTTTATGCCAAGTG